ADVANCED MATERIALS
www.advmat.de

Revisiting the Role of Polysulfides in Lithium–Sulfur Batteries

Gaoran Li, Shun Wang, Yining Zhang, Matthew Li, Zhongwei Chen,* and Jun Lu**

Intermediate polysulfides (S_n, where n = 2–8) play a critical role in both mechanistic understanding and performance improvement of lithium–sulfur batteries. The rational management of polysulfides is of profound significance for high-efficiency sulfur electrochemistry. Here, the key roles of polysulfides are discussed, with regard to their status, behavior, and their corresponding impact on the lithium–sulfur system. Two schools of thoughts for polysulfide management are proposed, their advantages and disadvantages are compared, and future developments are discussed.

1. Introduction

Battery technology plays a pivotal role in response to the worldwide energy crisis by enabling efficient utilization of sustainable but intermittent energy sources such as solar and wind.[1] Lithium–sulfur (Li–S) batteries are an intriguing alternative to succeed the current dominant lithium-ion (Li-ion) batteries to support the fast-expanding energy demand.[2] By coupling highly abundant sulfur with metallic lithium, the Li–S system is able to output almost fivefold higher energy density at one-third the cost compared to its predecessor. The Li–S energy is generated through the electrochemical redox reaction between elemental sulfur and lithium sulfide (Li_2S) accompanied by a series of intermediate polysulfides (PS) in conventional ether-based electrolyte.[3] In spite of the significant improvements achieved in the past few decades, the state-of-the-art Li–S batteries are still not able to meet the requirements of commercial applications due to the low practical energy density and limited lifespan.

The widespread implementation of Li–S batteries faces three main barriers. First, the insulating nature and the volume variation of the active materials during the charge–discharge result in impeded sulfur electrochemistry and fragile electrode integrity during cycling.[4] Second, the employment of highly reactive lithium metal induces severe electrolyte decomposition and dendrite formation, which lead to serious safety issues such as internal short circuits, heat accumulation, and gas evolution.[5] Most importantly, the existence and behavior of intermediate PS, which is the most important difference between Li–S and other battery systems, contribute to an extremely complex sulfur electrochemistry. The PS intermediates not only dissolve in electrolyte, resulting in severe active material loss, but also shuttle back and forth between the electrodes, causing severe coulombic inefficiency, anode corrosion, and resultant fast cell failure.[6] Improved control of PS behavior is thus essential to achieving satisfactory electrochemical performance and the practical realization of Li–S batteries.

Most previous reviews have summarized the recent progress on the structural design for specific components of the Li–S configuration, including the sulfur electrodes, interlayers, separators, electrolytes, and anodes.[3a,7] However, the PS behavior and its effect on sulfur electrochemistry, battery operation, and Li–S scale-up for practical application are rarely addressed. This review revisits the PS in the Li–S system, focusing on its composition, evolution, and behavior, as well as its significance in sulfur electrochemistry and battery performance. We start with an introduction of the basic physicochemical properties of PS anions, followed by their states and evolution in Li–S configurations. A detailed discussion of the behavior of PS anions and their positive and negative contributions to sulfur electrochemistry is subsequently provided. At present, there are two schools of thought on handling the PS-related problems: one in which the PS is suppressed, and the other in which it is retained. Finally, we compare the strengths and weaknesses of these strategies, specifically in terms of commercialization, and propose future directions of PS management for improved Li–S practical performance.

2. PS Existence and Evolution

Polysulfides form a class of chemical compounds containing multiple sulfur atoms linked by covalent bonds. The high S—S bond energy of 265 kJ mol^{-1} determines the high tendency of sulfur atoms to form homoatomic chains and rings; hence, the polysulfides are easy to form and commonly found in nature.[8] Polysulfides mainly exist in two forms, i.e., organic polysulfides

Dr. G. R. Li, Prof. S. Wang
Nanomaterials and Chemistry Key Laboratory
Wenzhou University
Wenzhou 325027, P. R. China
E-mail: shunwang@wzu.edu.cn
Dr. G. R. Li, Dr. Y. N. Zhang, M. Li, Prof. Z. W. Chen
Department of Chemical Engineering
University Waterloo
Waterloo, Ontario N2L 3G1, Canada
E-mail: zhwchen@uwaterloo.ca
Dr. J. Lu
Chemical Sciences and Engineering Division
Argonne National Laboratory
Argonne, IL 60439, USA
E-mail: junlu@anl.gov
The ORCID identification number(s) for the author(s) of this article can be found under https://doi.org/10.1002/adma.201705590.

DOI: 10.1002/adma.201705590

and inorganic polysulfide anions, and their ubiquity plays an important role in global geological and biological sulfur cycles.[9] Organic polysulfides have been widely applied in traditional rubber, sealant, and adhesive industries due to their excellent mechanical properties. Meanwhile, the polysulfide anions (PS, the abbreviation in this review refers specifically to polysulfide anions) are attracting increasing academic interest for their critical roles in the burgeoning energy technology of Li–S batteries.[10]

The PS can be obtained through the cleavage of the S—S bond in elemental S_8 by strong nucleophiles such as sulfide.[10] An early report on PS synthesis can be traced to 1884, when sodium polysulfide was synthesized via chemical comproportionation between stoichiometric sulfur and sodium sulfide in a water–alcohol mixture.[11] As for PS in an electrochemical system, the soluble PS anions were first discussed by Coleman and Bates in 1968, when opaque red–black solution was obtained from the partially discharged Li/DMSO-$KClO_4$/S system.[12] The product solution was considered to contain lithium polysulfides according to their similar optical and spectral properties to the previously reported sodium and potassium polysulfides formed by chemical reactions.[13] Intrigued by the unique properties as well as the critical roles in sulfur electrochemistry, several investigations have been conducted to reveal the physical, chemical, and electrochemical nature of PS.[14] The PS "status," i.e., the existing states of PS involving the charge number, oxidization state, cluster level, and steric configuration, is complicated and ever-changing. The PS anions mainly exist in two forms, i.e., the singly charged radical monoanion $S_n^{\bullet -}$ and the dianion S_n^{2-}. These two forms of PS are generally symbiotic in solution and high-temperature melts through the chemical equilibrium

$$S_{2n}^{2-} \leftrightarrow 2S_n^{\bullet -} \quad (1)$$

Moreover, PS anions coexist with each other in disproportionation or comproportionation equilibria due to their close Gibbs free energies[15]

$$2S_n^{2-} \leftrightarrow S_{n+m}^{2-} + S_{n-m}^{2-} \quad (2)$$

$$S_{n+m}^{2-} \leftrightarrow S_n^{\bullet -} + S_m^{\bullet -} \quad (3)$$

These complex and ubiquitous PS equilibria make it extremely difficult to isolate and characterize individual PS species analytically or spectroscopically. Computational calculations prefer the chain-like sulfur cluster over cyclic or chair-like geometries of PS anions in solutions due to their higher thermodynamic stability, which is also supported by extensive experimental results.[10,14] Furthermore, the high activity of the outer-shell electrons in the intermediate valence sulfur results in the high chemical reactivity of PS, which is manifested by their high sensitivity to air and moisture.[16] More importantly, the PS status is highly subject to solvent selection. For instance, the dominant stable PS species in aqueous solution are S_4^{2-} and S_5^{2-}, while higher order S_6^{2-} and S_8^{2-} show much higher stability in polar nonaqueous solutions such as tetrahydrofuran (THF), dimethoxyethane (DME), and dimethyl sulfoxide (DMSO).[17] The broad range of sulfur atom numbers in PS contributes to its wide range of molecular polarities, resulting in a strong dependence of PS solubility on solvent properties, as well as the simultaneous difficulty in searching for a solvent with universal solubility for all the PS anions.[18]

In Li–S batteries, well-selected organic liquid electrolytes are generally employed to support sulfur electrochemistry. The lithium polysulfides emerge as intermediate products during the charge–discharge process, whose status, evolution, and the corresponding impact on Li–S operation are critical in pursuit of good battery performance. Extensive experimental

Shun Wang is a distinguished Professor at the College of Chemistry and Materials Engineering, Wenzhou University. His research focuses on nanostructured functional materials, including carbon-based nanocomposites, functional Te nanocrystals, and hierarchically structured and assembled materials for electrochemical energy storage and conversion technologies.

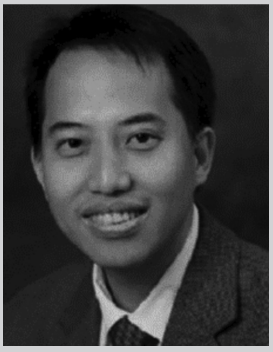

Zhongwei Chen is Canada Research Chair Professor in Advanced Materials for Clean Energy at the University of Waterloo, Waterloo, Canada. He received his Ph.D. degree in chemical and environmental engineering from the University of California Riverside in 2008. His expertise is advanced energy materials for zinc–air batteries, lithium-ion batteries, lithium–sulfur batteries and fuel cells.

Jun Lu is a chemist at Argonne National Laboratory. His research interests focus on electrochemical energy storage and conversion technology, with a main focus on beyond-lithium-ion battery technology. He received his bachelor's degree in chemistry physics from the University of Science and Technology of China (USTC) in 2000. He completed his Ph.D. from the Department of Metallurgical Engineering at the University of Utah in 2009 with major research on metal hydrides for reversible hydrogen storage application.

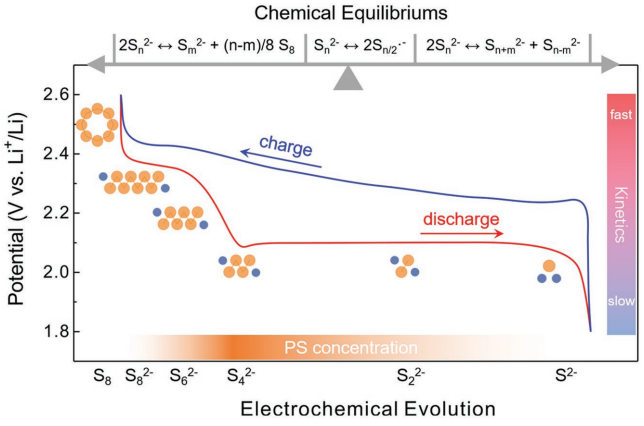

Figure 1. The compendium of PS composition and evolution in Li–S batteries.

measurements combined with computational simulations have made great contributions to the elementary identification of PS in nonaqueous electrolytes. Though PS anions with varied sulfur atom numbers are always symbiotic, S_8^{2-}, S_6^{2-}, S_4^{2-}, S_2^{2-} dianions and the $S_3^{\cdot-}$ radical monoanion have been well detected as the prominent existing state of PS.[17b,18,19] However, the aforementioned strong dependence of PS stability on solvent properties dictates the PS status in different electrolytes. In particular, electron pair donor solvent such as DMSO, dimethylacetamide (DMA), and dimethylformamide (DMF) are found to facilitate the stabilization of $S_3^{\cdot-}$ radical, while the $S_3^{\cdot-}$ radical is barely detectable in glyme-based electrolyte such as DME/dioxolane (DOL).[20] Moreover, density functional theory (DFT) calculations indicate the high tendency of lower-order Li_2S_4 to cluster or dimerize into Li_4S_8, while higher order Li_2S_6 and Li_2S_8 prefer monomeric units in DMSO solvent.[21] Notably, the PS solubility also varies dramatically in different electrolytes, e.g., ether-based electrolyte such as THF holds a high sulfur solubility up to ≈10 M, whereas carbonate electrolytes such as ethylene carbonate (EC), propylene carbonate (PC), and diethyl carbonate (DEC) can barely dissolve PS anions and even irreversibly consume PS via nucleophilic reactions.[17b,22]

Evolution of the PS status along with the electrochemical redox process is critical for the mechanistic understanding of sulfur electrochemistry. In recent years, theoretical calculations and extensive characterizations have been devoted to building up reference databases for PS identification during the electrochemical sulfur evolution.[23] However, the high air/moisture sensitivity and the ubiquitous chemical equilibria of PS anions cause serious difficulties in status detection. In this case, in situ/operando characterizations are strong methods to overcome these difficulties and realize the real-time and precise detection for the PS evolution. In situ/operando measurements, including Raman, X-ray diffraction, transmission X-ray microscopy, UV–vis spectroscopy, high performance liquid chromatography, equivalent series resistance, and X-ray absorption near edge structure (XANES), have produced a good compendium of PS evolution.[23b,24] The discharge process is started with the ring opening of S_8, followed by the PS reduction from high-order to low-order clusters ($S_8^{2-} \rightarrow S_6^{2-} \rightarrow S_4^{2-}$), and it ends with the deposition of Li_2S_2/Li_2S. The cell charging follows a reverse PS evolution to that in discharge (**Figure 1**). Additionally due to the varied PS stability in different solvent, the $S_3^{\cdot-}$ radicals are also an important intermediate equilibrating with S_6^{2-} anions in electron-donor solvent (such as DMSO, DMA, and DMF) based electrolytes, which shows a characteristic blue/green color rather than the typical yellow/brown color in conventional electrolytes that based on solvents with low donor number such as THF, DME, and DOL.[20]

The chemical equilibria in the Li–S system have also been uncovered upon battery operation. For instance, the detection of S_6^{2-} in the very early discharge is attributed to the PS disproportionation of $S_8^{2-} \leftrightarrow S_6^{2-} + 1/4S_8$, while the emergence of Li_2S in the middle of the second discharge voltage platform can be referred to the disproportion of S_4^{2-} and S_2^{2-} anions.[25] Moreover, the PS stability dependence on electrolyte properties also strongly influence the PS evolution. The sulfur electrochemical reaction pathways are guided by PS chemical equilibria toward more stable PS status, resulting in a varied distribution of PS anions in different electrolytes during the charge–discharge process.[26] Operando XANES provides strong support for this by revealing qualitative and quantitative variations of sulfur species in different electrolytes (**Figure 2**).[20,27] The species

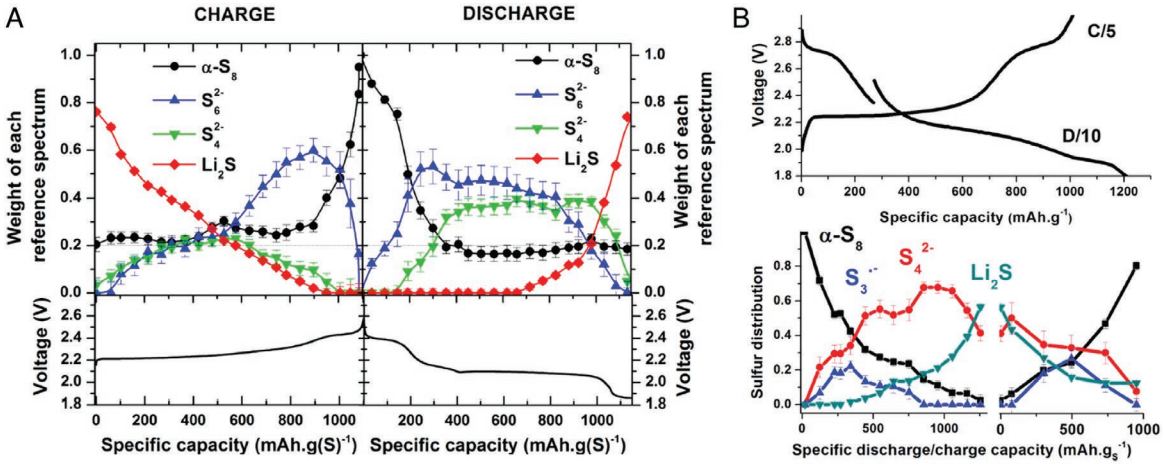

Figure 2. A,B) Evolution of sulfur K-edge XANES upon electrochemical cycling in DEM/DOL-based electrolytes (A) and DMA-based electrolytes (B) based on linear combination analysis. A) Reproduced with permission.[27] Copyright 2013, American Chemical Society. B) Reproduced with permission.[20] Copyright 2015, Wiley-VCH.

S_8 was found to be decreased as expected at the beginning of cell discharge in both DME/DOL- and DMA-based electrolyte. However, S_8 stabilized at a certain low content during the low-potential discharge in DME/DOL, while S_8 can be completely consumed in DMA electrolyte. The high stability of $S_3^{\bullet-}$ in DMA solvent is considered to strengthen the comproportionation between S_8 and S^{2-} to form $S_3^{\bullet-}$, leading to enhanced S_8 utilization.

3. PS Behavior and Effects

Apart from the complexity of PS composition and evolution, PS behavior (including dissolution, diffusion, shutting, and anodic corrosion) has a crucial influence on Li–S battery operation and electrochemical performance. The problems caused by the PS behavior have been considered as one of the most critical in pursuit of high sulfur utilization and stable sulfur electrochemical redox for Li–S batteries.

3.1. Disadvantages of PS Behavior

The PS behavior and the correspondingly resultant problems for battery operation and performance can be summarized into several intertwined phenomena. Upon discharge, the electroreduction of elemental sulfur on the electrode's surface generates high-order soluble PS species (e.g., S_8^{2-} and S_6^{2-}), which then proceed to be solvated by the electrolyte. The sulfur phase variation from solid to liquid causes contact loss between binder and active materials, as well as subsequent electrode structural collapse.[28]

Subsequently, the PS species diffuse from the cathode surface into the electrolyte bulk, through the porous separator, and permeate into the anode section. The concentration gradient determines that sulfur species cannot be fully recaptured by the cathode, leading to irreversible sulfur loss.[29] Moreover, the accumulation of PS in electrolyte causes considerable increases in viscosity, while the PS chemical disproportionation produces insulative Li_2S_2/Li_2S precipitates, leading to porosity loss in both the cathode and separator.[28a,30] These behaviors result in severely hindered ion transfer and increased cell impedance.

As the PS species diffuse to the anode, the highly active PS species are chemically reduced on the lithium surface, generating irreversible Li_2S_2/Li_2S deposition and leading to further sulfur loss, severe self-discharge, and impeded ion/electron transfer for Li redox. Particularly in charge process, the soluble long-chain PS generated in cathode migrate to the anode chamber and are chemically transformed into short-chain PS, which subsequently diffuse back to cathode and electrochemically oxidized back into long-chain PS species.[31] Thus, the PS shuttling back and forth between electrodes, i.e., the so-called "shuttle effect," causes severe coulombic loss, continuous anode corrosion, amplified electrolyte decomposition, and low sulfur utilization.

Furthermore, the PS dissolution, diffusion, and deposition cause unceasing variations of electrolyte viscosity, electron/ion conductivity, and sulfur phase states during the battery cycling. These, in turn, lead to an ever-changing internal resistance as well as great difficulty in attaining sustainable sulfur electrochemistry in the Li–S configuration.[32]

In addition to these problems, PS behavior is considered as the main culprit in the low sulfur utilization and fast cell failure for Li–S batteries. These problems are even more severe when sulfur electrochemistry is implemented in similar energy technologies, e.g., ambient-temperature sodium–sulfur battery, which are aimed at overcoming the serious safety, reliability, and maintenance issues in commercialized sodium–sulfur batteries based on ceramic solid electrolyte and high temperature operation (over 300 °C).[33]

3.2. Advantages of PS Behavior

Although the aforementioned PS behavior has caused serious troubles for Li–S batteries, the PS participation in the sulfur electrochemistry is not readily replaced. This is because PS also brings very favorable effects to the Li–S system.

Most importantly, PS chemical equilibria play active roles in producing a thorough and fast sulfur redox reaction through enhanced kinetics (**Figure 3**). Upon discharge, the PS dissolution exposes the inner parts of the sulfur particles, which are originally less reachable for both electrons and ions, thus acquiring enhanced sulfur utilization. Moreover, the PS species are able to drag the insulating sulfur into electrolyte via chemical comproportionation, e.g., $S_8 + S_4^{2-} \rightarrow S_6^{2-}$. The generated PS can be easily reduced on the conductive host surface, while active sulfur is redistributed on the electrode surface with easier access to both electrons and ions. Consequently, the PS participation favors solid–liquid sulfur conversion and electrochemical redox on the electrode/electrolyte interface, overcoming the much higher electron/ion transfer resistance within the bulk sulfur in pure solid sulfur electrochemistry.[34] A similar effect also occurs upon the charge process, where the PS chemical equilibria help to catalyze the oxidation of Li_2S, e.g., $Li_2S + S_6^{2-} \rightarrow S_4^{2-}$, by overcoming the activation energy for PS nucleation.[35] These superior properties are strongly supported by the significantly smaller electrochemical impedance and higher output voltage in the PS-dissolved liquid Li–S configuration than those based on pure solid sulfur redox.[32] Besides, the comproportionations between the reduced (S_2^{2-} or S^{2-}) and oxidized (S_8 or S_8^{2-}) species can also improve the utilization of the leftover sulfur species during the cycling, leading to a more thorough sulfur electrochemical redox.[20] Interestingly, the rotating ring disk electrode experiments performed by Lu et al. indicated only a $4e^-$ electrochemical route for sulfur electrochemical reduction, much less than that in the theoretical $16e^-$ route ($S_8 + Li + 16e^- \leftrightarrow 8Li_2S$), suggesting that complete sulfur conversion can only be accomplished through the cooperative combination of chemical and electrochemical processes.[36]

The sulfur phase conversion homogenizes the sulfur distribution in the electrode during cycling for improved utilization. Inhomogeneous sulfur distribution fails to fully utilize the conductive surface and renders large aggregates that easily lose electrical/ionic contact, thus leading to inactivation of sulfur solids and continuous capacity loss. Therefore, the persistently uniform sulfur distribution in electrode is of great significance to achieve high-efficiency and reversible sulfur electrochemistry. The PS anions intrinsically generated upon the battery cycling are able to relocate sulfur to where

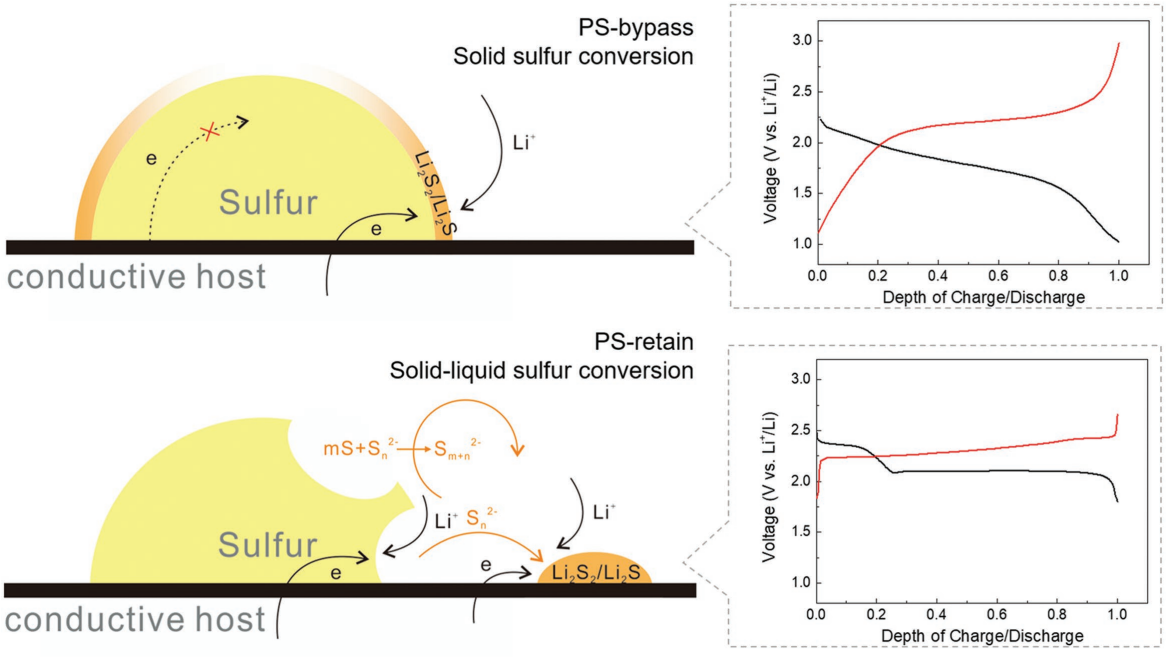

Figure 3. Illustration of the sulfur electrochemistry and the corresponding voltage profile (top) without and (bottom) with PS participation.

with easier access to electron and ion by the equilibrium-driven solubilization of the inert sulfur solids and their migration to the electric/ionic active spots due to the high mobility of PS anions. The continuous and repetitive dissolution-deposition process facilitates the uniform sulfur redistribution as commonly seen as the "activation process" with continuous capacity increase upon the early cycles in literatures.[37] Beyond that, researches also uncovered the great benefit of extrinsically PS-contained electrolyte in promoting the sulfur redistribution. The preloaded and persistently high-concentration PS anions in electrolyte serve as the "healing agent" to mitigate the spatial heterogeneity of PS on electrode surface, which mediates the sulfur phase variation and lead to the uniform nucleation and growth of solid compounds.[38] The high-efficiency and durable sulfur redistribution enables significantly improved reaction kinetics, enhanced sulfur utilization, and prolonged lifespan.

Beyond that, PS is also favorable for prolonging the battery lifespan by participating in the formation of a protective layer on the lithium surface. Inhibition of lithium dendrite formation is reported when employing coupled additives of PS and $LiNO_3$ in electrolyte.[39] Based on a competition mechanism, $LiNO_3$ could first react with lithium metal to form a passivation layer to reduce the chemical reaction between PS and lithium, while Li_2S/Li_2S_2 mainly forms in the upper layer of the solid-electrolyte interphase (SEI) to minimize the electrolyte decomposition, thus contributing to a prolonged cycling life and enhanced coulombic efficiency. However, this mechanism may not be sufficiently powerful considering the fast failure of high-sulfur-loading batteries, which may relate to the regulation on the PS concentration in electrolyte as well as the applied current density.[39]

In summary, PS behavior can be considered a double-edged sword for Li–S batteries, both improving and damaging Li–S electrochemistry. The manipulation on PS behavior to take advantage of the positive over the negative effects is of great significance in pursuit of good Li–S battery performance.

4. Two Schools of Thought for PS Management

In view of the abovementioned dual PS character in the Li–S system, the choice of PS management can be divided into two different schools of thought: the PS-bypass and PS-retain strategies. The PS-bypass strategies aim to completely avoid the existence of PS anions in the Li–S configuration, thereby escaping from the serious problems they can cause. In contrast, PS-retain strategies advocate conserving PS species to take advantage of their positive contributions, but regulating the PS behavior through advanced material and structural designs to inhibit the shuttling effect.

4.1. PS-Bypass Designs

Numerous research efforts have been devoted to bypassing PS species for prolonged battery lifespan.[40] The key idea of these strategies is to eliminate the formation of PS at its source. Since the PS species in Li–S batteries are generated in forms of dissolved anions induced by the interactions between sulfur and solvent molecules, the cathode and electrolyte designs for cutting off these interactions follow two main directions: one focusing on the cathode, and the other, the electrolyte.

4.1.1. Cathode Strategies

Electrode structural design for bypassing PS behavior has been the research emphasis for Li–S batteries. Representatively, by

confining small sulfur allotropes (S_{2-4}) inside a microporous (<0.5 nm) carbon matrix, PS generation can be successfully avoided due to spatial restriction preventing the unfavorable transition between S_8 and S_4^{2-} (**Figure 4**A).[41] Li et al. improved this mechanism and proposed that the lost contact between sulfur species and electrolyte solvent due to the steric hindrance of electrolyte penetration is responsible to the elimination of PS dissolution. In this condition, both the electron and ion transfers are dependent on the microporous carbon matrix (Figure 4B).[42] These spatial selections against the sulfur–electrolyte interaction yield a solid-state sulfur electrochemistry, which is embodied by a single-plateau discharge curve at lower potential compared to the typical two-plateau profile in conventional Li–S batteries. Sulfurized organics, represented by sulfurized polyacrylonitrile (SPAN, Figure 4C), is also an attractive alternative for the PS-bypass cathode design. The sulfur short chains are covalently anchored on the cyclized, partially dehydrogenated, and ribbon-like PAN backbones. The sulfur electrochemistry is realized by breaking S—S bonds while the chain ends are immobilized in the PAN skeleton, thus resulting in the elimination of PS dissolution. Meanwhile, the conductive polyacetylene-like backbone is capable of offering a satisfactory electron supply for sulfur electrochemical redox.[43] Similarly, Yang's group proposed a carbyne polysulfide with a conducting sp2 hybrid carbon skeleton connecting to the short sulfur side chain (Figure 4D). The covalently anchored short-chain sulfur performs a solid-phase electro-reduction to form Li_2S and Li_2S_2 without the generation and dissolution of long-chain PS anions.[44] Recently, Zhou et al. reported an interesting PS-bypass strategy by using selenium as bridge linking the short-chains polysulfides that were grafted on the polymer skeleton for enhanced conductivity and eliminated PS shuttling (Figure 4E). The obtained organosulfur electrode showed impressive volumetric and coulombic efficiency.[45] Benefiting

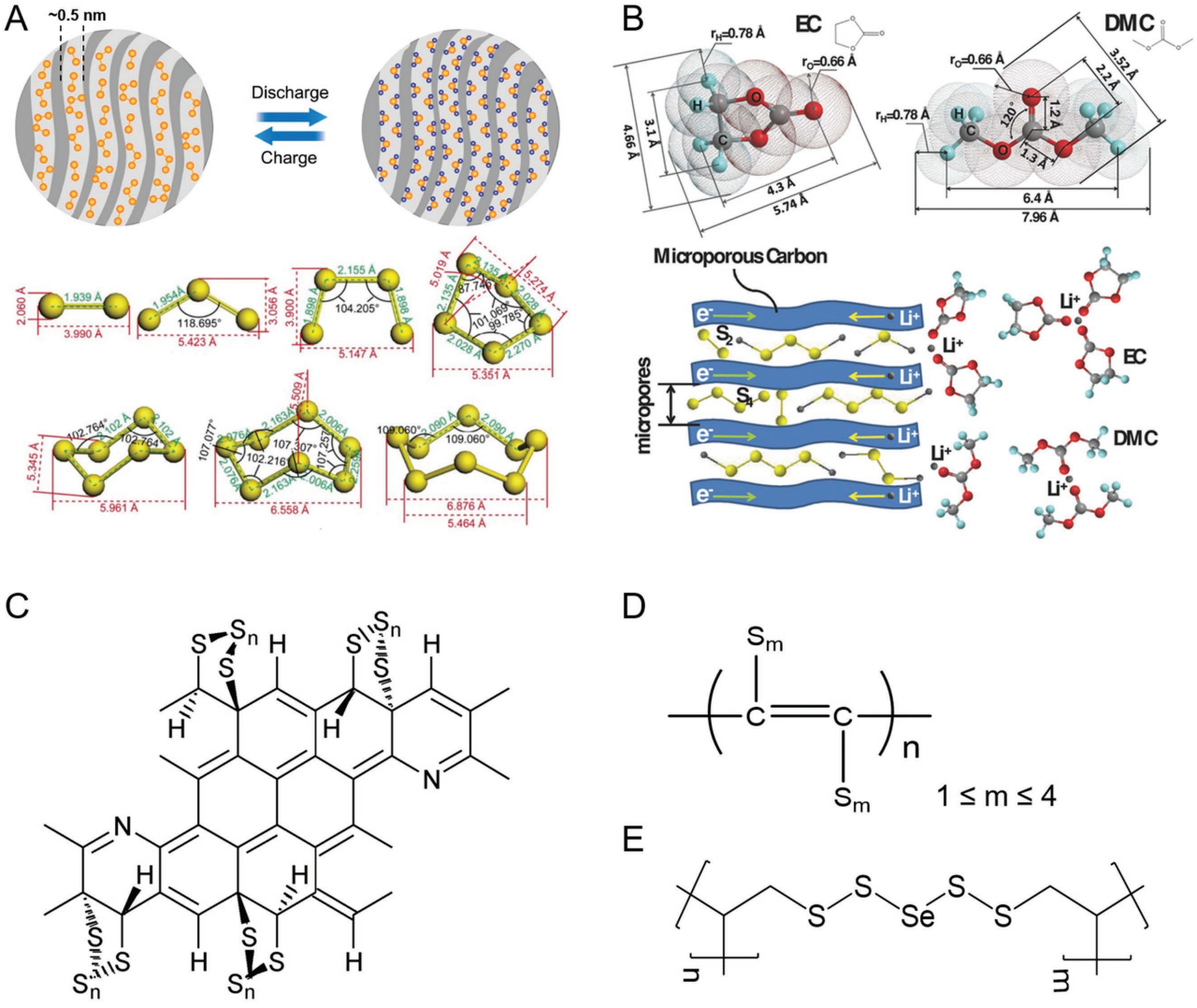

Figure 4. A) Schematic of the spatial confinement for small sulfur charge–discharge. Reproduced with permission.[41] Copyright 2012, American Chemical Society. B) Schematic of the lithiation process of sulfur/microporous carbon cathode in carbonate electrolyte. Reproduced with permission.[42] Copyright 2013, Wiley-VCH. C–E) Proposed chemical structures of SPAN (C), carbyne polysulfide (D), and selenium-doped organosulfur (E). C,D) Reproduced with permission.[44] Copyright 2013, Royal Society of Chemistry. E) Reproduced with permission.[45] Copyright 2017, Wiley-VCH.

from these factors, PS-bypass electrode designs could reach up to an ultrahigh cyclability over 4000 cycles with negligible capacity fading.[46]

More importantly, the superiority of these PS-bypass electrode designs lies in the availability of carbonate electrolyte in the corresponding Li–S configurations. As the most commonly used electrolyte in commercial Li-ion batteries, carbonate electrolyte delivers competitive conductivity, lower cost, and higher safety than conventional ether-based electrolyte.[47] Unfortunately, the carbonates fail to support general Li–S batteries due to their chemical incompatibility with PS anions, which trigger severe sulfur loss, electrolyte decomposition, and fast cell failure.[22] These PS-bypass electrode designs effectively avoid the irreversible nucleophilic reactions between PS and carbonates, and have thus revived interest in the employment of carbonate electrolyte for cheaper, scalable, and reliable Li–S batteries.

Some criticism of the PS-bypass electrode designs has arisen due to their relatively low sulfur content (generally <50 wt%).[43a,48] The microporous carbon host fails to accommodate large amounts of sulfur due to its generally low pore volume, while the sulfur content in organic sulfides is also unsatisfactory due to the limited sulfur grafting. The low sulfur content strongly restricts these PS-bypass electrodes from yielding satisfactory energy density for practical use.

4.1.2. Electrolyte Strategies

Another pathway toward the PS-bypass configuration relies on electrolyte improvements. Since the negative PS behavior is initiated by PS dissolution, electrolyte substitution that eliminates sulfur solubility is considered as a straightforward solution to eradicate this problem. However, due to the broad polarity range of polysulfides as well as their vulnerability to nucleophilic attacks, it is extremely hard to develop liquid electrolytes that can not only insolubilize polysulfides but also simultaneously dissociate the lithium salts in a high-efficiency way, which is also the reason why successful PS-bypass strategies focusing on liquid electrolyte designs have barely been reported.[18]

Solid-state electrolytes (SSEs) have been widely recognized as the ultimate solution for future battery technologies due to their excellent safety performance, including high chemical, electrochemical, thermal, and mechanical stabilities.[49] In the case of the Li–S battery, SSE enables the absolute absence of PS dissolving liquid solvents, which realizes a complete avoidance of PS dissolution and shuttling. Moreover, the substitution of SSE over liquid electrolyte can suppress the formation of lithium dendrites, as well as prevent electrolyte leakage, volatilization, and combustion, leading to greatly improved Li–S battery safety (**Figure 5**).

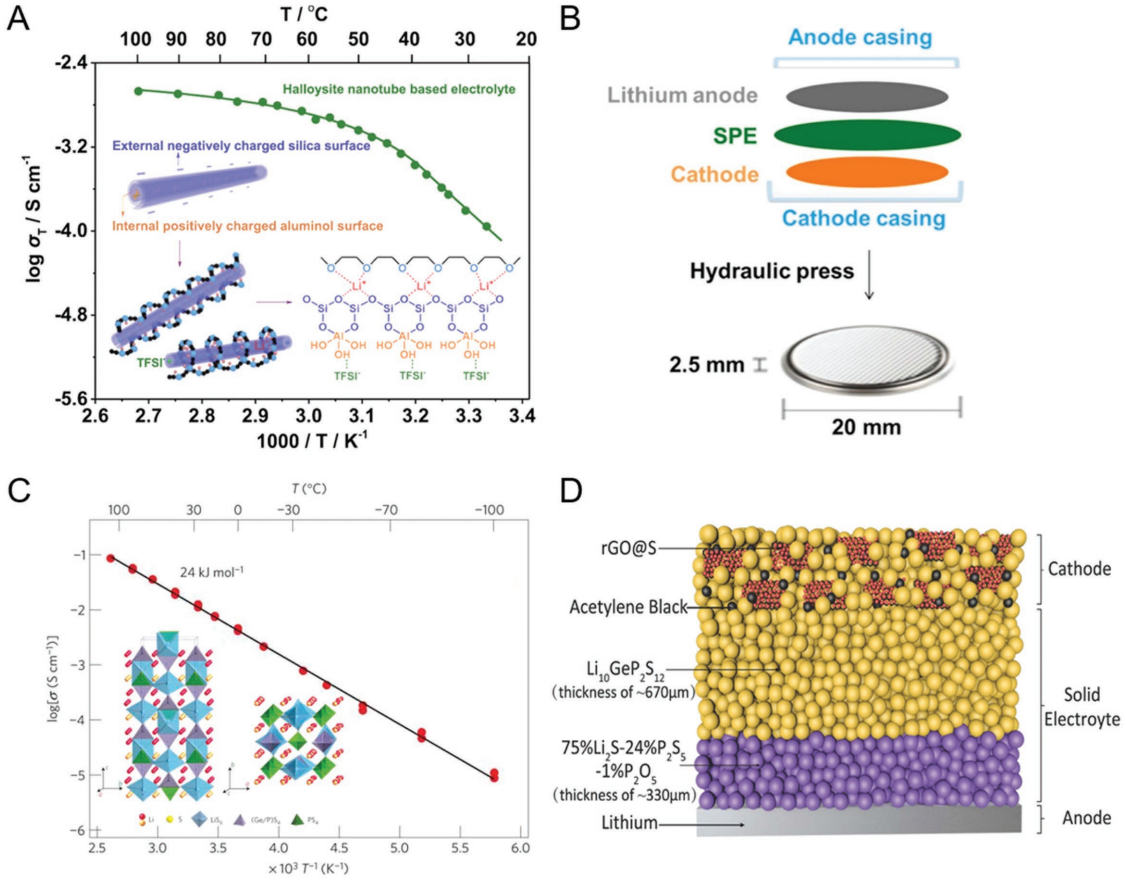

Figure 5. A) The ion conductivity and structure of SPE based on halloysite nanotubes, poly(ethylene oxide) (PEO), and lithium bis(trifluoromethane sulfonyl) imide (LiTFSI). B) Schematic diagram of an all-solid-state Li–S battery based on SPE electrolyte. Reproduced with permission.[50b] Copyright 2016, Elsevier Ltd. C) The ion conductivity and crystal structure of $Li_{10}GeP_2S_{12}$. Reproduced with permission.[52a] Copyright 2011, Nature Publishing Group. D) Schematic diagram of an all-solid-state Li–S battery based on $Li_{10}GeP_2S_{12}$ electrolyte. Reproduced with permission.[53] Copyright 2017, Wiley-VCH.

Polyether, as a representative solid polymer electrolyte (SPE), has shown promise in Li–S batteries. The coordination between Li^+ in the lithium salt and the sequential oxyethylene in the polyether favors the dissociation and dissolution of Li^+ to offer decent ion conductivity for sulfur electrochemistry.[50] The impregnation of inorganic ceramic fillers, such as Al_2O_3, SiO_2, and ZrO_2, has been widely explored to further enhance the ion conductivity of polymer SSE by reducing the crystallinity of the polymer solvent and the resistance of the electrode/electrolyte interface.[51] Meanwhile, inorganic SSE delivering potentially higher ion conductivity is expected to provide faster electrochemical kinetics for solid Li–S batteries. Top-performing Li^+ superconductors, such as $Li_{10}GeP_2S_{12}$, $Li_{9.54}Si_{1.74}P_{1.44}S_{11.7}Cl_{0.3}$, $Li_{10}(Ge_{0.5}Sn_{0.5})P_2S_{12}$, and Li_2S-P_2S_5, have been reported to exhibit appealing Li^+ conductivity of 10^{-2}–10^{-3} S cm^{-1} at ambient temperature, which is comparable to that of commercial liquid electrolytes.[52] By coupling nanosulfur/reduced graphene oxide composite and $Li_{10}GeP_2S_{12}$ electrolyte, solid-state Li–S was endowed with outstanding cyclability over 750 cycles at 60 °C.[53] The nanosize effect of uniformly distributed active sulfur significantly reduces the stress/strain during the lithiation/delithiation process, while the effective PS bypassing and strong ion support from the inorganic electrolyte attain sustainable and fast sulfur electrochemistry; their combined effect ultimately results in extended battery lifespan. However, the problems involving poor compatibility with the lithium metal, high interface impedance, air/moisture sensitivity, and high cost are still hindering SSE from large-scale manufacturing and high battery performance.[54] In addition, the large occupation of carbon and SSE in the electron/ion supply results in a low sulfur content in the electrode, which is a major obstruction to the solid-state Li–S battery from yielding satisfactory energy density for practical use.

4.2. PS-Retain Designs

In comparison to PS-bypass designs, a promising alternative is the less radical methods of retaining PS species in the Li–S configuration with rational regulation of their behavior. The PS-retain strategies conserve the positive contributions of PS behavior producing fast and efficient sulfur electrochemistry, and also exert considerable inhibition of PS shutting, thereby minimizing its harmful effect on battery operation. The PS regulation in the Li–S configuration can be achieved by several methods, including PS confinement, dissolution inhibition, blocking, and side reaction inhibition (**Figure 6**), as discussed further below.

4.2.1. PS Confinement

The PS confinement is mainly realized by immobilizing PS species within cathodes via physical and/or chemical adsorptions so as to achieve an inhibited shuttling effect. Carbon materials have attracted the most research enthusiasm as the sulfur host due to their excellent structural plasticity, high porosity, excellent conductivity, and light weight. Multiple dimensional carbon constructions with various morphologies have been widely investigated, serving as conductive agents as well as physical absorber to PS anions (Figure 6A).[7b,55] Apart from physical confinement, polar hosts such as heteroatom-doped carbon,[56] conductive polymers,[57] and metal oxides/sulfides/nitrides/carbides[58] have been evidenced capable of offering favorable PS confinement via chemical interactions such as "lithium bonding" (similar to hydrogen bonding) and electrostatic attraction between oppositely charged active sites in PS and host materials.[59] Similarly, polar binders other than the conventional poly(vinylidene fluoride) (PVDF) binder have also been revealed to strengthen chemical adsorption to PS species, as well as improve electrode integrity for stabilized sulfur electrochemistry.[60] Beyond the adsorption mechanism, the implementations of polar materials also favors the enhancement of reaction kinetics for sulfur electrochemistry. The polar materials hold strong chemical affinity to PS anions thus to anchor them on the conductive substrate for facilitated reception of electric and ionic supplies. Such effects also contribute to a raised local concentration of PS anions and further accelerate the sulfur heterogeneous electro-redox.[61] The expedited sulfur electrochemistry not only serve as an indirect sulfur confinement due to the fast sulfur precipitation and limited PS diffusion, but also favors the electrochemical performance under high sulfur loading where the reaction kinetics are critical limitations.[62] Apart from that, recently advances in organo-polysulfides are also promising approaches toward inhibited polysulfide shuttling by covalently attaching active sulfur on the polymeric skeleton.[63] Talapaneni et al. reported a covalent triazine framework (CTF) chemically impregnated with sulfur as active materials for Li–S batteries.[64] Through an in situ vulcanization between CTF and sulfur, the obtained organopolysulfide was endowed with covalent attachment of sulfur as well as homogeneous sulfur distribution within the pores. Importantly, the covalent bondage and the spatial constraint in CTF offers favorable confinement to PS, thus enabling inhibited PS shuttling and improved battery cyclability. Similarly, Yan's group use cysteamine as the bridge to covalently combine sulfur copolymer with graphene nanosheets.[65] Attributed to the covalent sulfur stabilization, the formation of long-chain PS anions and the PS shuttling behavior were significantly inhibited. Although considerable improvements of battery performance have been achieved through various PS confinement strategies, it is worth noting that no matter how strongly the PS is confined, the existence of PS in these PS-retain configurations still disallows the use of carbonate electrolyte due to sensitive nucleophilic reactions.

4.2.2. PS Dissolution Inhibition

All the behaviors and subsequent problems associated with PS can be traced back to the initial dissolution of PS. Hence, the inhibition of PS dissolution is considered as one of the most straightforward solutions toward improved Li–S cyclability. Unlike the carbonate electrolyte and SSE used in PS-bypass designs, mild solvent manipulation focusing on the PS-solvent interaction to inhibit PS dissolution is a promising method to balance the positive and negative contributions from PS behavior.[66] Inspired by the benefits of fluoroethylene carbonate in Li-ion battery system, fluorinated ethers such as 1,1,2,2-tetrafluoroethyl-2,2,3,3-tetrafluoropropyl ether, 1,3-(1,1,2,2-tetrafluoroethoxy) propane, bis(2,2,2-trifluoroethyl) ether, etc., have been extensively studied

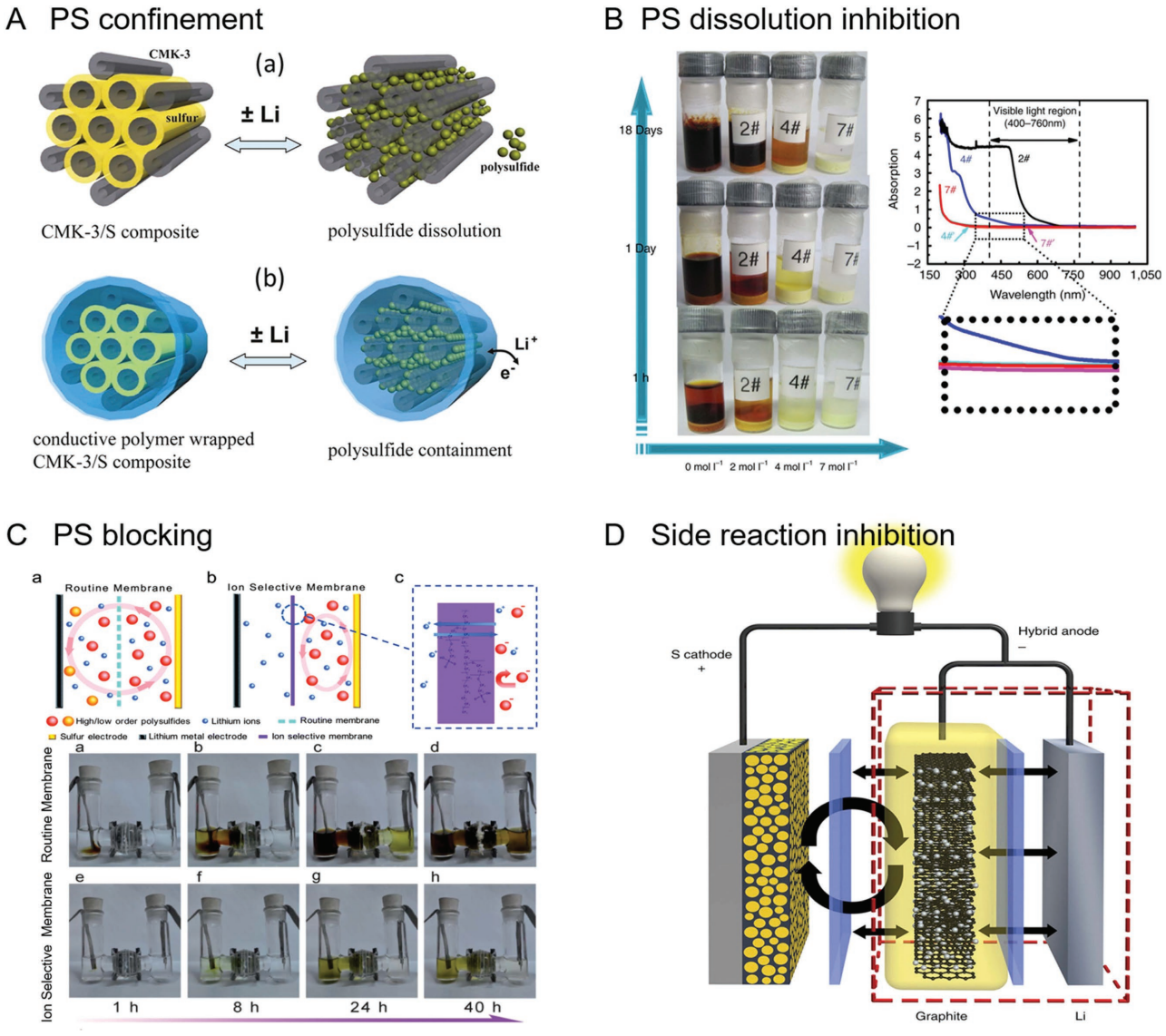

Figure 6. PS regulation attained by PS-retain strategies: A) confining PS within the cathode by porous carbon and conductive polymer wrapping, B) inhibiting PS dissolution by a highly concentrated electrolyte, C) blocking PS penetration by a separator coated with an ion-selective polymer, and D) protecting the lithium anode from PS corrosion with graphite layer. A) Reproduced with permission.[55b] Copyright 2011, American Chemical Society. B) Reproduced with permission.[71] Copyright 2013, Nature Publishing Group. C) Reproduced with permission.[76] Copyright 2016, Nature Publishing Group. D) Reproduced with permission.[88] Copyright 2014, Nature Publishing Group.

as cosolvent or additive for conventional electrolyte to suppress the PS dissolution due to their low donor-ability and poor solvation to PS anions, along with a combined protective interfaces on both cathode and anode.[67] Interesting works were reported by Nazar's group using an $(ACN)_2$-LiTFSI-hydrofluoroether blend as electrolyte for Li–S batteries.[68] Since most of the acetonitrile (ACN) molecules are effectively bound with the lithium salts by forming the 2:1 complex, such electrolyte design not only circumvents the potential incompatibility between ACN and metallic lithium, but also significantly suppresses the dissolution of PS anions as well as their mobilities due to the sparing solvation. However, these benefits are accompanied by the reduced dissolution and ionization of lithium salts, resulting in deterioration of ion conductivity and reaction kinetics. To address this problem, they further developed a new electrolyte by coupling *N,N*-dimethyl triflamide (DMT) and $Li[Al(Ohfip)_4]$ as solvent and lithium salt, respectively.[69] The DMT molecules holding highly electron-withdrawing groups and deactivated Lewis basic sites are barely PS-dissolving, while the highly disassociated $Li[Al(Ohfip)_4]$ rather than LiTFSI are able to offer decent ion conductivity in such solvent environment to support the electrochemistry. Almost nonsolvation to polysulfide can be realized at ambient temperature under such electrolyte design (though the formation of PS species is still detected), while the sparing PS dissolution and significantly inhibited PS shuttling are still achievable at raised temperature of 50 °C.

Apart from that, recent progress has revealed the great efficacy of concentrated electrolyte in taming PS shuttling.[70]

A "solvent-in-salt" electrolyte with an ultrahigh salt concentration up to 7 M has been found to significantly reduce the PS dissolution realized by the common ion effect (Figure 6B).[71] The increased competition between the solvation to TFSI and PS anions contributes to reduced PS dissolution, thus leading to inhibited PS shuttling, enhanced coulombic efficiency, and improved cycling stability. Based on similar idea of weak PS solvation, well-selected ionic liquids (ILs) are found also effective in reducing PS dissolution and prolonging cycling stability.[72] The employment of IL electrolytes additionally improves the cell safety due to its inherent nonvolatility and nonflammability. Yet, IL-based electrolytes are still severely restricted in Li–S batteries owing to their expensiveness, hygroscopicity, high viscosity, and limited ion conductivity.[73] Apart from ILs, gel or hybrid electrolytes have also been extensively investigated in order to combine the merits of liquid and solid electrolytes for improved cyclability and acceptable rate capability.[74] Beyond these manipulations on electrolyte, researchers also developed some ingenious functionalization that favors inhibition on PS dissolution for improved Li–S battery performance. Huang's group applied a biological catalyst dithiothreitol serving as the PS scissor to slice the S—S bonds in long-chain PS, thus rapidly eliminating the accumulation of dissolvable PS anions and effectively inhibiting the PS dissolution as well as the PS shuttling.[75]

4.2.3. PS Blocking

The shuttling effect relies on the PS diffusion between electrodes; hence, the suppression of PS diffusion also serves as an effective method for PS management. Interlayer/separator designs, as a typical instantiation of PS blocking strategies, have recently experienced an extraordinary rise in popularity among Li–S battery developers. By building up an ion selective layer between the electrodes, the PS penetration from cathode to anode can be effectively blocked, contributing to a significant inhibition of PS shuttling. Zhou's group recently reported a metal-organic framework (MOF)-based battery separator to manipulate the PS diffusion in Li–S batteries. The highly ordered micropores in MOF crystals offer a suitable size window, enabling the MOF-based separator to selectively sieve Li^+ ions while efficiently blocking the undesired PS penetration from cathode to anode (Figure 6C).[76] Similar PS shields can be realized by anion-repelling or size-selective polymers and inorganics,[77] as well as the direct use of a solid-state electrolyte layer as separator.[78] Apart from that, interlayers between the cathode and conventional separator containing PS absorber such as carbon materials,[79] metal oxides/sulfides/carbides/nitrides,[75,80] and functional polymers[81] can provide effective PS resistance by capturing and reutilizing PS anions. Beyond that, the employments of polar materials in functional interlayers also contribute to an enhanced electrochemical reaction kinetics, thus to realize an improved regulation on PS migration.[80,82] Zhang's group constructed a cooperative interface by combining "lithiophilic" nitrogen-doping graphene and "sulfiphilic" NiFe layered double hydroxide (LDH) as the functional interlayer for Li–S batteries.[83] The synergistic chemical attraction to PS anions enriches their local concentration for fast kinetics, while the Fe doping and the metal–nitrogen interaction induce the stressed strain within LDH lattice, which serve as a high-efficiency catalyst for the heterogeneous sulfur electro-redox. The catalyzed sulfur conversions facilitate the precipitations of sulfur species within the cathodic section, thus significantly suppresses the PS migration to lithium anode. More importantly, such catalysis also favors smooth and reliable sulfur electrochemistry in high-sulfur-loading configurations, which has long been plagued by their poor kinetics.[62a,84]

4.2.4. Side Reaction Inhibition

Side reactions on the lithium's surface are another critical source for PS shuttling and fast battery failure. These detrimental reactions not only cause severe sulfur consumption and low coulombic efficiency, but also induce drastic anode corrosion, enhanced cell impedance, and serious safety concerns.[85] Anode engineering is an important pathway toward eliminating side reactions for improved electrochemical and safety performance. Protective layer construction and anode substitutes are typical methods for anode engineering. Stable and reliable barriers against PS attack and dendrite formation can be built up through in situ SEI strengthening by optimized electrolyte[86] and ex situ protection constructed by artificial layer formation.[87] Huang et al. incorporated a hybrid anode consisting of electrically connected graphite and lithium metal in a PS-retain configuration to manipulate the anode surface reaction.[88] The lithiated graphite protection on the lithium surface serves as a self-regulated SEI layer to resist PS attack and smooth the Li^+ transfer, leading to a considerable alleviation of side reactions (Figure 6D). Functional electrolyte additive is an effective approach toward stable lithium anode. When $LiNO_3$ has been widely applied in Li–S configurations to form an N-rich protective anode SEI,[89] PS anions are found also favorable in mitigating anodic side reactions. The passivation contributed by the reaction products between PS anions and metallic lithium serve as a protective interface to inhibit the decomposition of electrolyte on lithium surface.[90] Beyond that, such protection layer can be further strengthened by the synergistic cooperation between PS and $LiNO_3$ additives due to the formation of a compact, stable, and S,N dually rich SEI, which not only impedes the excessive electrolyte decomposition and the lithium dendrite formation, but also offers enhanced Li^+ conductivity for faster electrochemistry.[39,91] The PS concentration in the dual-additive electrolyte is critical for the stability of the in situ formed SEI since a highly concentrated PS (>0.5 M for S) fails to maintain a smooth and firm anode surface.[92] Recently an interesting work was presented by Wang's group using organo-polysulfide as electrolyte additive for stable lithium anode.[93] The poly(sulfur-random-triallylamine) takes participation in anode SEI formation by generating both inorganic Li salts (Li_2S/Li_2S_2) and organic units. The organic units serve as a "plasticizer" in the SEI to improve its flexibility and toughness, while the inorganic units provide Li conductive pathways. With such a synergistical hybridization, the obtained Li–S batteries shows inhibited PS shuttling, stabilize lithium anode, and excellent cycling stability.

Anode substitution can be regarded as a more straightforward solution for the side reaction problem. By replacing

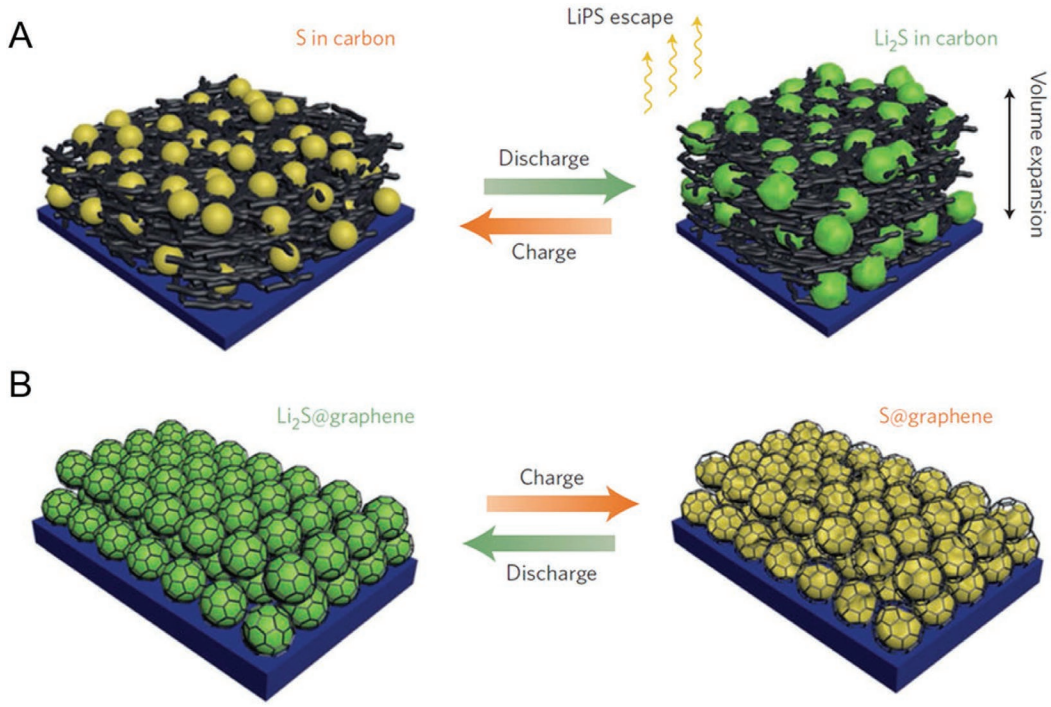

Figure 7. A) The conventional hybrid sulfur cathodes with elemental sulfur dispersed over a porous and electrically conductive scaffold such as a carbon-based structure. B) The Li_2S-based cathode design with Li_2S nanoparticles compactly and seamlessly encapsulated by graphene to achieve high volumetric efficiency and high sulfur loading (sulfur: yellow spheres; Li_2S: green spheres). Reproduced with permission.[97b] Copyright 2017, Nature Publishing Group.

metallic lithium with less reactive anode materials such as graphite,[88] silicon,[94] carbon group metals,[95] and alloys,[96] considerable improvement in cycling stability can be achieved owing to the elimination of Li-PS side reactions, though some of these alternatives need antecedent prelithiation to compensate the lithium use before coupling with element sulfur cathode. In addition, these anode substitution sacrifices the power and energy density of Li–S batteries since most of these alternatives result in higher electric potential and less specific energy than those of lithium metal. Moreover, the nonlithiated anode materials must rely on a lithiated sulfur cathode (Li_2S) to introduce sufficient lithium ions into the system. The Li_2S cathodes offer several intrinsic advantages for enhanced battery performance. As the fully lithiated phase of sulfur species, the use of Li_2S can successfully eliminate the volume expansion for improved electrode integrity.[34] More importantly, the significantly higher thermal stability of Li_2S over elemental sulfur enables easier material engineering for compactly and seamlessly encapsulated active sulfur, thus leading to inhibited PS dissolution, enhanced volumetric efficiency, and consequently, higher mass loading (**Figure 7**).[97] Nevertheless, the air/moisture sensitivity and expensiveness of Li_2S are still strongly limiting its utilization by considerably increasing the manufacturing complexity and cost.[34]

4.2.5. PS Catholyte

As an extreme PS-retain strategy, PS catholyte-based batteries have recently drawn an increased amount of research attention. By using PS-contained catholyte, controlled voltage cutoff, and pretreated lithium anode, a PS-based flow battery is realized with a decent energy density of 108 Wh L^{-1} and excellent cyclability over 2000 cycles (**Figure 8**).[98] When coupling PS catholyte and an alternative iodide anode, the redox flow battery can achieve high energy and a notably low cost of \$85.4 (kW h)$^{-1}$, which is almost half that of the state-of-the-art vanadium-based flow battery, making it an attractive prospect in large-scale stationary electrical applications.[99] As in coin-cell configurations, chemically prepared PS catholyte can be applied as the active materials for high-performance Li–S batteries. By taking advantages of the uniform PS distribution and their fast interfacial reactions, the combination of PS catholyte and highly porous conductive host holds good access to high sulfur loading and decent redox kinetics for Li–S batteries, though the negative effects of PS-retain designs may become more serious due to the flooding of PS anions.[28b,100] Beyond that, liquid organopolysulfide was revealed with distinctive electrochemistry as catholyte for Li–S batteries. Chen et al. recently presented a very interesting work by using a functional dimethyl disulfide (DMDS) as catholyte as well as the electrolyte cosolvent for Li–S batteries.[101] When coupled with sulfur/carbon cathode, an adequate DMDS was capable of quickly dissolving element sulfur to form an equilibrate mixture of soluble dimethyl polysulfides ($CH_3SS_mSCH_3$, m = 1 or 2), which circumvents the generation of long-chain PS anions accompanied by a lowered discharge plateaus, and simultaneously activates the electrochemical activity of the sulfur covalently bonded in DMDS molecules to provide additional capacity (Figure 8D,E). Similar progress was also achieved by Fu's group, who used

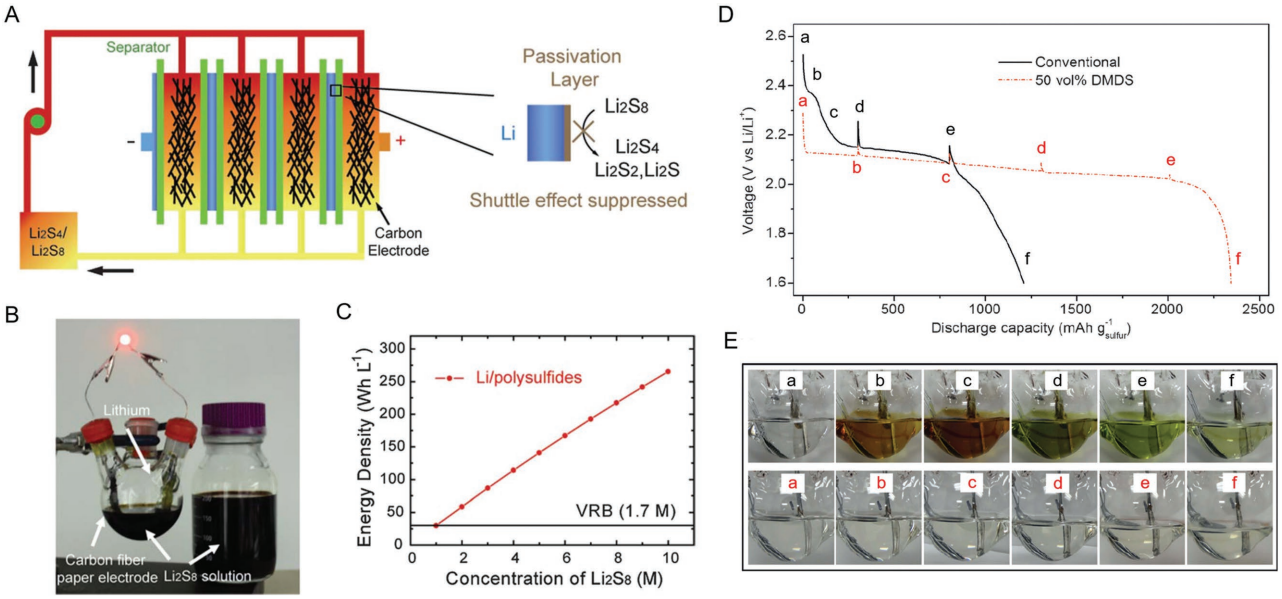

Figure 8. A) Schematic illustration and B,C) experimental demonstration of the Li–PS catholyte flow battery. A–C) Reproduced with permission.[98] Copyright 2013, Royal Society of Chemistry. D) Initial discharge profiles of the flask cells with conventional (black) and 50 vol% DMDS-containing (red) electrolyte. E) Electrolyte color changes at corresponding points in (D) during discharge. D,E) Reproduced with permission.[101] Copyright 2016, Wiley-VCH.

dimethyltrisulfide as catholyte to pair with pure carbon electrode and perform high-efficiency and reversible sulfur electrochemistry with discharge product of $LiSCH_3$ and Li_2S.[102] It should be noted that although these organo-polysulfides-containing catholytes are able to significantly reduce the conventional PS anions in the corresponding battery configurations, electrochemically or chemically active S—S bond are still in dissolved states in electrolyte, which can also induce side reactions with metallic lithium and irreversible energy loss.

These PS-retain strategies have undoubtedly achieved considerable improvement in capacity and cyclability for Li–S batteries. A qualitative comparison between PS-bypass and PS-retain strategies is given in **Table 1** in terms of different electrochemical and battery properties. In general, PS-retain strategies tends to achieve faster kinetics, higher capacity, higher output voltage, and easier access to high sulfur content/loading, but poorer anode sustainability and cycling stability compared to those in the PS-bypass configurations. The PS-bypass management was committed to the eradication of PS dissolution through electrode and electrolyte manipulations, thus to cut off the source of PS shuttling and achieve characteristically high reversibility and durability of sulfur electrochemistry. However due to the intrinsically poor electronic and ionic conductivity of sulfur and its lithiated products, as well as the absence of solid–liquid interfacial reactions, the solid-state sulfur conversions in PS-bypass designs suffer from sluggish kinetics, low sulfur utilization, and poor rate capability. Therefore, blind pursuit of bypassing PS in current Li–S mechanism may results in considerable sacrifice of energy and power densities. Improvement of the reaction kinetics for solid sulfur electrochemistry is an urgent research topic for PS by-pass strategies. The development of new pathways for sulfur electrochemical conversion, which involves novel sulfur-based materials and/or sulfur-solvent coordination, are necessary to circumvent the poor conductivity of active materials in the state-of-art Li–S chemistry.

Table 1. Comparison between PS-bypass and PS-retain strategies.

	PS-bypass[a,b)]	PS-retain[a,b)]
Kinetics	–	+
Capacity	–	+
Cyclability	+	–
Anode sustainability	+	–
Voltage output	–	+
Sulfur content/loading	–	+

[a)]+: superior; [b)]–: inferior.

By contrast, the PS-retain strategies conserve the solution chemistry of PS in Li–S system but with specific regulations against PS behavior in purpose of effective inhibition on detrimental PS shuttling. The dissolution of PS introduces the solid–liquid sulfur conversion into the Li–S system, where the sulfur phase transition and the PS chemical equilibria contribute to much easier access to electron and ion as well as uniform sulfur distribution within the electrode, therefore enabling a significantly fastened sulfur electrochemistry. However, considerable drawbacks of PS-retain strategies also require serious concerns. The conservation of PS dissolution in PS-retain configurations inevitably results in irreversible sulfur loss in electrolyte, while the accompanying PS shuttling behavior still causes irreversible sulfur consumption and chemical/electrochemical corrosion in anode. Meanwhile, considerable amount of electrolyte is required to support the solution chemistry of PS, which augments the resistance for Li–S batteries to yielding high energy density particularly in high-sulfur-loading conditions. Functional interlayer/separator and anodic surface designs are of particular significance in future development

of PS-retain Li–S batteries, which are responsible to build up ion selective shield to block PS diffusion and simultaneously provide satisfactory Li^+ conductivity, thereby to well balance the positive and negative contributions of PS behavior. Moreover, electrode and electrolyte designs targeting to sparing electrolyte usage is another critical aspect that need more research efforts in purpose of achieving satisfactorily high energy density for commercial application.

5. PS in High-Loading Li–S Batteries

Extensive explorations and investigations have been devoted to study the PS composition, behavior, and their impacts on battery operation. Encouraging progress in energy density, lifespan, and operational reliability of Li–S batteries has been achieved via rational PS management. However, a huge gap still remains between the state-of-the-art battery performance and the commercial standards. Specifically, when evaluating Li–S batteries on the basis of the mass and volume parameters of the entire prototype rather than the sole sulfur electrode, which needs to take into account all the battery shells, electrodes, electrolytes, etc., the seemingly excellent performances reported in the literatures are considerably diminished since they are generally obtained under low sulfur loading and excessive lithium and electrolyte. Moreover, the common use of lithium metal and low-boiling solvents in the PS-bypass and PS-retain strategies also presents serious potential safety hazards. Therefore, significant progress is needed to boost the practical battery performance. In view of the distinctive sulfur electrochemistry in PS-bypass and PS-retain strategies, the obstacles, the developing tactics, and the potential applications also differs on their ways to high energy storage and future commercialization.

5.1. PS-Bypass for High-Loading Li–S Batteries

It can be deduced from the above discussion that PS-bypass compared with PS-retain designs are more adept at prolonging battery lifespan by annihilating PS shuttling. This superiority may favor applications such as microelectronics, which prefers operation stability over ultrahigh energy. However, the inadequacies of sulfur loading, high cost, low energy density, and poor electrochemical kinetics are serious obstructions to the large-scale application for PS-bypass strategies. The progress on PS-bypass strategies for high-loading Li–S batteries relies on breakthroughs in sulfur-based material science for novel sulfur-rich active materials, or sulfur electrochemistry with faster reaction pathways. Transition metal sulfides and polysulfides are promising candidates to achieve sulfur electrochemistry with enhanced sulfur loading due to higher tap density. Metal sulfides/polysulfides have been widely reported with decent lithium and sodium storage in carbonate-based electrolytes, indicating their good PS bypass operation.[103] The current understanding of the lithiation mechanism for metal sulfides is generally reported to include Li_2S formation in a low-potential conversion process.[104] However, the inevitable generation of PS anions from the delithiation of Li_2S phase is expected to occur, and these anions will react irreversibly and detrimentally with carbonates via nucleophilic reactions. This apparent contradiction between the observed good cyclability and the current mechanistic understanding deserves further exploration so as to offer effective guidance for material engineering to power PS-bypass Li–S batteries with higher mass loading and energy density. Apart from that, the solid-state configuration is also promising alternative for high-energy PS-bypass Li–S batteries. The development of SSE with higher conductivity and easier fabrication is expected to support higher sulfur loading and enhanced energy output.

5.2. PS-Retain for High-Loading Li–S Batteries

Compared with PS-bypass strategies, the current PS-retain designs deliver superior capability with respect to fast and efficient sulfur electrochemistry, but relatively limited cycling stability. The superiority of PS-retain designs endows them with greater promise in high energy/power applications such as electric vehicles, power stations, and smart grids. When sulfur loading is raised to commercially viable scales, the PS-retain strategies possess an overwhelming advantage over the PS-bypass strategies in attaining high capacity. The majority of the recent breakthroughs for high-energy Li–S batteries is realized in PS-retain systems with advanced electrode construction or interlayer designs. Rationally designed PS-retain configurations have been reported to be accessible to high sulfur loading even up to >60 mg cm^{-2} and cathodic sulfur content over 80 wt%,[62a,105] while PS-bypass designs have barely achieved acceptable sulfur loading and energy density.[40,43a] In spite of their easier access to high sulfur loading and energy density, significant problems still remain in PS-retain strategies, as explained below.

5.2.1. Amplified PS Behavior

The development of advanced PS-retain high-loading batteries requires a large amount of PS (i.e., PS-flooding) but with good diminishment of the PS-retain negative impacts. The high PS concentration in batteries drastically increases the electrolyte viscosity and subsequently reduces electrolyte wettability and conductivity, leading to deteriorated reaction kinetics.[106] Moreover, the raised current density also severely accelerates the corrosion and dendrite formation in the lithium anode, leading to higher internal impedance and fast cell failure. These PS-related problems make the PS management strategies more important to high-loading sulfur electrodes that are stable. Although numerous attempts have been made to resolve the much-amplified negative PS effects in these sulfur-rich configurations, thus far very limited cyclability has been reported in tests under commercially appropriate sulfur loading. The PS management in PS-flooding batteries relies on the cooperative contribution from every battery constituent. The facile and low-cost electrode constructions with self-standing property, highly porosity, and long-range conductivity are promising to overcome the deteriorated electrochemical impedance in PS-flooding batteries. Surface functionalization, e.g., by polar materials for enhanced affinity to PS and catalyzed sulfur

electrochemistry may also favor the suppressed PS shuttling and decreased internal impedance. Particularly, the development of high-sulfur-loading electrodes requires additionally volumetric rather than only areal evaluation in order to offer more reliable reference for their potentially practical applications. Moreover, functional separator/interlayer designs assist in restricting PS anions that escape from the cathode. Future work on PS barrier designs should focus more on achieving a smooth Li^+ penetration to ensure adequate Li^+ supply. Single-ion conducting polymers and SSE are promising candidates but are only feasible if, and only if, the poor ion conductivities are addressed. Anode engineering should be oriented to strengthening the inhibition of dendrite formation and electrolyte decomposition. Rational design of a Li^+-conducting layer on the lithium surface with facile preparation and robust protection is promising to retain the superiority of the lithium anode in PS-flooding batteries.

5.2.2. Electrolyte Amount

Electrolyte amount is a critical factor for Li–S battery performance. Electrolyte abuse has been a serious problem in current Li–S development. The majority of the reported excellent performance is obtained under electrolyte-to-sulfur (E/S) ratios over 10 mL g^{-1}, which not only raises the cost but also leads to increased battery weight and less energy density. Hagen et al. conducted a contrastive calculation and set forth an E/S standard of 3/1 (mL g^{-1}) for Li–S batteries to achieve competitive cost and energy density to conventional Li-ion batteries in 18 650 prototype.[107] Such an index has barely been reported in literatures. However, it is worth noting that such small electrolyte usage is bound to cause extremely high PS concentration and amplified PS negative behavior in Li–S configuration. The E/S ratio of 3 mL g^{-1} corresponds to a sulfur concentration of ≈10.5 M, which surpasses the PS saturation in conventional electrolyte even in form of the most dissolvable PS, i.e., S_8^{2-}.[108] These considerations orient to the problems posed by ultrahigh PS concentration and solid-state sulfur electrochemistry, which analogizes the defects in PS-bypass strategies and may lead to drastic performance degradation. Hence, electrolyte development aiming at even higher PS solubility in the premise of good Li^+ conductivity and effective PS management may be a promising pathway toward reduced electrolyte addition and satisfactory practical performance. In-depth and systematic understanding of PS behavior under low E/S ratio also deserves continuous investigation to guide the further development of high-energy Li–S batteries.

5.2.3. Electrolyte Decomposition

Electrolyte decomposition is another critical aspect that is often neglected in the development of advanced PS-retain configurations. The decomposition of the electrolyte contributes to the SEI formation, but the nonhomogeneous plating of lithium creates a very unstable SEI, which constantly consumes electrolyte. This unceasing electrolyte depletion and gas evolution lead to long-term capacity decay, increased internal impedance, and serious safety hazards.[89,109] The PS anions play a significant role in the electrolyte decomposition, typically represented by the irreversible nucleophilic reactions between PS and carbonates. Beyond that, ether solvent is also vulnerable to the nucleophilic attack from $S_3^{\cdot-}$ radical and short-chain PS anions, similar to the electrolyte consumption induced by the superoxide attack in the Li–O_2 battery.[20,110] These PS-involved electrolyte decompositions could be intensified by the PS flooding in high-sulfur-loading prototypes. The aforementioned anode protections are helpful in inhibiting electrolyte decomposition. More effective experimental methods as well as a deeper understanding of the electrolyte decomposition mechanism in PS-flooding configuration are needed.

5.2.4. Resistance to Harsh Conditions

Resistance to harsh conditions is a critical battery performance indicator for practical use. In particular, the sensitivity of Li–S battery performance to temperature is a great challenge. The significant deterioration of PS solubility, electrolyte viscosity, and ion conductivity in PS-flooding batteries under low temperature (e.g., <10 °C) results in a dramatic performance degradation. Meanwhile, the low boiling point of ether-based electrolyte raises serious safety concerns at higher temperature. Beyond that, the ability of Li–S batteries to resist a catastrophic failure during severe mechanical deformation, high/low pressure, and puncture also requires considerable research attention. Future development of Li–S batteries should pay more attention to the behavior of PS during these harsh conditions, so as to achieve high tolerance and reliability of Li–S operation in real-world circumstances.

6. Toward Practically Viable Li–S Batteries

With the Li-ion batteries approaching their theoretical limits as well as the fast development of Li–S battery technology, the commercialization of Li–S batteries is increasingly expected to revolutionize the energy market attributed to their low cost and high energy density. Sulfur is one of the most abundant elements on the earth, and also geographically well-distributed and highly environmentally benign, which endows it with an intriguingly low cost that is only 0.5% of the conventional cathode material (**Table 2**). In spite of the relatively higher prices of metallic lithium and electrolyte, Li–S batteries still hold promisingly less than one-fourth the price per kilowatt-hour of Li-ion batteries in a cell level, showing great advantage as a cost-effective candidate for future energy storage.

When the electrochemical performances in literatures are dominantly evaluated based on the mass or volume of element sulfur or cathode, capacities and energy densities in the cell level are more critical and valuable in assessing the practical viability of Li–S batteries. Given this, we summarized the critical parameters and performances of the representative Li–S pouch cells as shown in **Table 3**. Academic attempts with high sulfur loading and sparing electrolyte in Li–S pouch cells are capable of yielding energy density of 300–400 Wh kg^{-1} under several ampere-hours scale. Meanwhile, the industry pioneers, such as Oxis Energy Ltd. and Sion Power Corp., have demonstrated their Li–S products with competitive energy densities to their

Table 2. Cost comparison between Li-ion and Li–S batteries.[2b,111]

	Unit	Li-ion		Li–S	
Cathode	\$ kg^{-1}	$LiCoO_2$	40	S	0.2
Binder	\$ kg^{-1}	PVDF	10	PVDF	10
Anode	\$ kg^{-1}	Graphite	12	Li	50
Separator	\$ m^{-2}	PP/PE/PP	2	PP/PE/PP	2
Electrolyte	\$ L^{-1}	$LiPF_6$/EC:EMC	18	LiTFSI/DME:DOL	50[a)]
Current Collector	\$ m^{-2}	Al	0.8	Al	0.8
		Cu	1.8	–	–
Cell cost	\$ $(kW\ h)^{-1}$	600		<150	

[a)]Estimated based on the prices of components.

Table 3. Parameters and performance of Li–S pouch cells with capacity over 1 Ah.

	Capacity [Ah]	Gravimetric energy density [Wh kg^{-1}]	Volumetric energy density [Wh L^{-1}]	Cyclability	Sulfur loading [mg cm^{-2}]	E/S [mL g^{-1}]	Ref.
Chen et al.	1	470	300	40	4	2.5	[112]
Qu et al.	4	350		35	3	4	[113]
Xue et al.	5	350	300	80–100	4.5–6.5	3	[114]
Chen et al.	1.55	315	–	50	7.56	2.7	[115]
Cheng et al.	1.5	–	<200	100	4.43	3	[116]
Salihoglu and Demir-Cakan	3	120	–	<100	9.2	8	[117]
Ma et al.	10	504	654	Primary	>6	>3	[118]
Oxis	19.5	300	228	100	–	–	[119]
Sion	–	350	310	30–50	–	–	[120]

commercialized Li-ion opponents particularly in gravimetric aspect. These research efforts have shown the great promise of Li–S in realizing practically high energy density. However, it should be noted that the cyclabilities of these Li–S pouch cells are still severely limited compared with Li-ion batteries. Considering the great room for improvement, we further carried out a cell-level energy-density calculation in pouch cell configuration with sulfur loading and E/S ratio as variables, trying to uncover their impacts on battery energy densities as well as the potential competitiveness of Li–S batteries in energy storage market. The calculation is based on the following conditions:

- The densities of sulfur, lithium sulfide, carbon, and lithium refer to their basic physical properties. The thicknesses of cathode and anode layers are calculated based on their mass loading and densities. The space for sulfur volume variation (80%) is reserved in cathode;
- The areal densities and thickness of aluminum foil and aluminum–plastic package refer to commercial standards. No copper foil is used for anode;
- The sulfur content in cathode composite is 80 wt%;
- The densities of electrolytes are 1 g cm^{-3};
- The nominal cell voltage is 2.15 V;
- Sulfur performs a capacity of 1200 mAh g^{-1}, and lithium excess is 50%;
- The pouch cell contains 20 stacks of the unit as boxed in red in **Figure 9**A;
- The mass and volume of the tabs and extra package are ignored.

Figure 9B,C shows the gravimetric and volumetric energy densities of Li–S pouch cell respectively along with the variation of sulfur loading and E/S ratio under the calculation conditions. The dark dash lines present the DOE targets (250 Wh kg^{-1} and 400 Wh L^{-1}, respectively).[121] It could be perceived that Li–S batteries are easier to achieve the DOE goal in gravimetric level attributed to the light weight and high specific capacities of both sulfur and lithium. However, the Li–S configuration shows weakened volumetric advantage as a result of the low tap densities of sulfur, carbon, and lithium. A high-level volumetric energy density can only be achieved under a much lower E/S ratio and higher sulfur loading compared with those for the gravimetric energy-density goal. Significantly, the sulfur loading and E/S ratio are two of the most critical indexes for practically viable Li–S batteries. The increase of sulfur loading and decrease of E/S ratio clearly contribute to improved energy density for Li–S pouch cell. The coupling of 6 mg cm^{-2} sulfur loading and 3.5 mL g^{-1} E/S ratio, which seems achievable in the state-of-art technical conditions, results in gravimetric and volumetric energy densities of 408.2 Wh kg^{-1} and 402.2 Wh L^{-1} respectively under our calculation model and meets the DOE standards, though a compromise in performance may be involved when it comes to real operation. Moreover, the contribution of lowering the electrolyte use is noted becoming increasingly prominent in energy enhancement when approaching to the high-energy-density level, as perceived from the tangent under constant energy density in the surface plot represented by the DOL goal line. Therefore, the rational management of electrolyte amount in

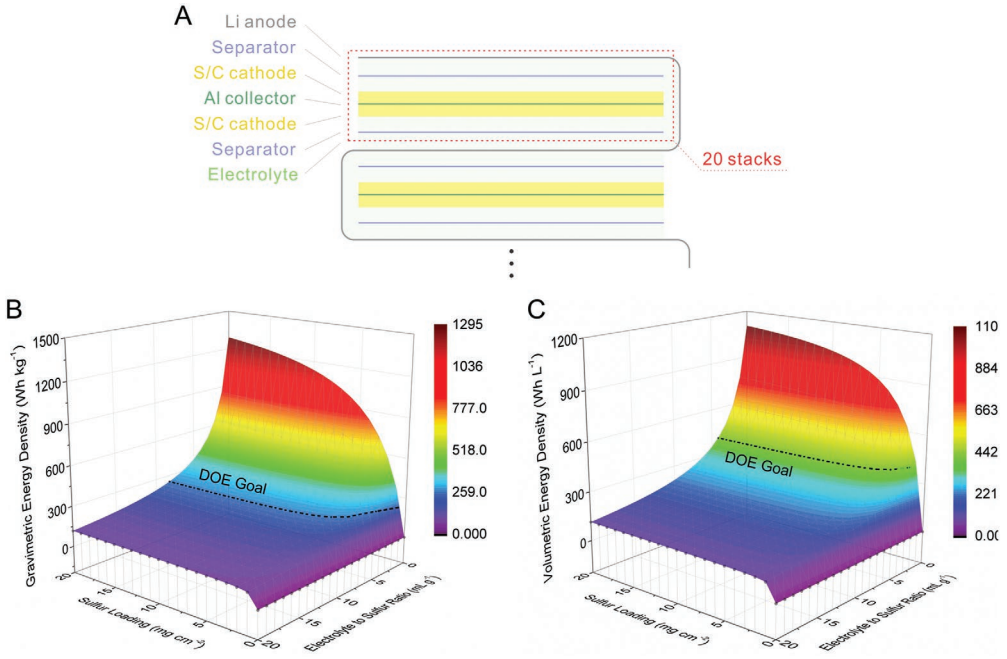

Figure 9. A) Sketch of the stacking in an Li–S pouch cell. B,C) Calculated gravimetric (B) and volumetric (C) energy densities of a Li–S pouch cell depending on sulfur loading and electrolyte-to-sulfur ratio.

battery configuration is particularly important for the achievement of high energy density. However unfortunately, while quite a number of literatures have reported high sulfur loadings that satisfied the requirements as demonstrated in this calculation, very few publications integrated with the accordingly low E/S ratio to ensure practically high energy density in cell level. This may be ascribed to the ineluctable requirement of considerable amount of electrolyte to wet the electrodes and separator, and more importantly to support the solution-based sulfur electrochemistry as discussed in above sections. Therefore, future research efforts need focus more on the sparing use of electrolyte in order to achieve practically viable Li–S batteries, which may involve the development of new electrolyte system and improvement in solid-based sulfur electrochemistry. Beyond that, the cyclability of the Li–S chemistry in practical prototype is still very limited (Table 3), which is another critical barrier for its commercialization. The desired improvement calls for not only the rational designs of sulfur electrode and electrolyte, but also smart anode engineering as mentioned above, which serves as another nonnegligible developing direction, and may as well benefit the safety management and tolerance to harsh environment for practical viable Li–S batteries.

7. Conclusion

Systematic study of the PS characteristics and behavior is paramount for the development of Li–S batteries to cater to the requirements of next-generation energy storage. The PS chemistry and electrochemistry in the Li–S system contribute to the intrinsic various valences, parasitic dynamic equilibria, and high chemical reactivity. In addition, the PS status, evolution, and behavior exert both positive and negative effects on sulfur electrochemistry and battery performance, which deserve critical evaluation and utilization in Li–S development.

The last few decades have witnessed a tremendous improvement in addressing PS-related problems. These attempts can be classified as PS-bypass and PS-retain strategies based on the choice of PS management strategy. The PS-bypass strategies eliminate PS behavior in Li–S batteries to attain excellent cyclability with low energy density, while the PS-retain strategies conserve PS species under certain conditions for improved sulfur utilization and fast reaction kinetics.

The rational retention or suppression of PS enables the development of competitive Li–S batteries in different fields of application. The highly reliable battery operation with the PS-bypass strategies is promising in low energy density applications such as microelectronics, while the PS-retain configurations hold huge potential to meet the high power and energy demands of the electric vehicle market. The many challenges and opportunities brought forward by PS in Li–S batteries are deepening our understanding of the underlying mechanism as well as bringing superior technology innovations. The realization of commercial Li–S batteries depends on collaborative contributions from the academic and industrial communities.

Acknowledgements

J.L. gratefully acknowledges support from the Assistant Secretary for Energy Efficiency and Renewable Energy, Office of Vehicle Technologies of the U.S. Department of Energy through the Advanced Battery Materials Research (BMR) Program (Battery500 Consortium). Argonne National Laboratory is operated for DOE Office of Science by UChicago Argonne, LLC, under contract number DE-AC02-06CH11357. The authors also acknowledge the financial support from the Natural

Sciences and Engineering Research Council of Canada (NSERC), the University of Waterloo, and the Waterloo Institute for Nanotechnology. S.W. gratefully acknowledges financial support from the National Natural Science Foundation of China (51272182, 51772219, 21471116, and 51641210), the Zhejiang Provincial Natural Science Foundation of China (LZ17E020002 and LZ15E020002), and the Wenzhou Scientific and Technological in Public Project (G20170018).

Conflict of Interest

The authors declare no conflict of interest.

Keywords

energy density, lithium–sulfur batteries, polysulfide management, polysulfides

Received: September 26, 2017
Revised: November 17, 2017
Published online:

[1] a) N. Savage, K. Bourzac, *Nature* **2017**, *545*, S13; b) B. Dunn, H. Kamath, J. M. Tarascon, *Science* **2011**, *334*, 928.
[2] a) R. F. Service, *Science* **2013**, *339*, 20; b) P. G. Bruce, S. A. Freunberger, L. J. Hardwick, J. M. Tarascon, *Nat. Mater.* **2011**, *11*, 19.
[3] a) A. Manthiram, Y. Fu, S. H. Chung, C. Zu, Y. S. Su, *Chem. Rev.* **2014**, *114*, 11751; b) Y. X. Yin, S. Xin, Y. G. Guo, L. J. Wan, *Angew. Chem., Int. Ed. Engl.* **2013**, *52*, 13186.
[4] Z. W. Seh, Y. Sun, Q. Zhang, Y. Cui, *Chem. Soc. Rev.* **2016**, *45*, 5605.
[5] D. Lin, Y. Liu, Y. Cui, *Nat. Nanotechnol.* **2017**, *12*, 194.
[6] A. Rosenman, E. Markevich, G. Salitra, D. Aurbach, A. Garsuch, F. F. Chesneau, *Adv. Energy Mater.* **2015**, *5*, 1500212.
[7] a) Q. Pang, X. Liang, C. Y. Kwok, L. F. Nazar, *Nat. Energy* **2016**, *1*, 16132; b) Y. Yang, G. Zheng, Y. Cui, *Chem. Soc. Rev.* **2013**, *42*, 3018.
[8] R. Steudel, *Chem. Rev.* **2002**, *102*, 3905.
[9] P. Lens, L. H. Pol, *Environmental Technologies to Treat Sulfur Pollution*, IWA Publishing, London **2000**.
[10] R. Steudel, *Elemental Sulfur and Sulfur-Rich Compounds II*, Vol. *2*, Springer Science & Business Media, New York **2003**.
[11] H. Böttger, *Eur. J. Org. Chem.* **1884**, *223*, 335.
[12] J. R. Coleman, M. W. Bates, presented at *Proceedings of the 6th International Symposium on Power Sources*, Brighton, September **1968**.
[13] F. W. Bergstrom, *J. Am. Chem. Soc.* **1926**, *48*, 146.
[14] D. L. Pringle, *PhD Thesis*, Iowa State University, **1967**.
[15] S. S. Zhang, *J. Power Sources* **2013**, *231*, 153.
[16] R. Steudel, G. Holdt, T. Gobel, *J. Chromatogr.* **1989**, *475*, 442.
[17] a) P. L. Cloke, *Geochim. Cosmochim. Acta* **1963**, *27*, 1265; b) R. S. Assary, L. A. Curtiss, J. S. Moore, *J. Phys. Chem. C* **2014**, *118*, 11545.
[18] S. Zhang, K. Ueno, K. Dokko, M. Watanabe, *Adv. Energy Mater.* **2015**, *5*, 1500117.
[19] R. P. Martin, W. H. Doub, J. L. Roberts, D. T. Sawyer, *Inorg. Chem.* **1973**, *12*, 1921.
[20] M. Cuisinier, C. Hart, M. Balasubramanian, A. Garsuch, L. F. Nazar, *Adv. Energy Mater.* **2015**, *5*, 1401801.
[21] M. Vijayakumar, N. Govind, E. Walter, S. D. Burton, A. Shukla, A. Devaraj, J. Xiao, J. Liu, C. Wang, A. Karim, S. Thevuthasan, *Phys. Chem. Chem. Phys.* **2014**, *16*, 10923.
[22] J. Gao, M. A. Lowe, Y. Kiya, H. D. Abruna, *J. Phys. Chem. C* **2011**, *115*, 25132.
[23] a) G. Zhang, Z. W. Zhang, H. J. Peng, J. Q. Huang, Q. Zhang, *Small Methods* **2017**, *1*, 1700134; b) M. Wild, L. O'neill, T. Zhang, R. Purkayastha, G. Minton, M. Marinescu, G. J. Offer, *Energy Environ. Sci.* **2015**, *8*, 3477; c) R. Xu, J. Lu, K. Amine, *Adv. Energy Mater.* **2015**, *5*, 1500408.
[24] a) J. Nelson, S. Misra, Y. Yang, A. Jackson, Y. Liu, H. Wang, H. Dai, J. C. Andrews, Y. Cui, M. F. Toney, *J. Am. Chem. Soc.* **2012**, *134*, 6337; b) J. Conder, R. Bouchet, S. Trabesinger, C. Marino, L. Gubler, C. Villevieille, *Nat. Energy* **2017**, *2*, 17069.
[25] a) C. Barchasz, F. Molton, C. Duboc, J. C. Lepretre, S. Patoux, F. Alloin, *Anal. Chem.* **2012**, *84*, 3973; b) Q. Wang, J. M. Zheng, E. Walter, H. L. Pan, D. P. Lv, P. J. Zuo, H. H. Chen, Z. D. Deng, B. Y. Liaw, X. Q. Yu, X. Q. Yang, J. G. Zhang, J. Liu, J. Xiao, *J. Electrochem. Soc.* **2015**, *162*, A474.
[26] Q. Zou, Y. C. Lu, *J. Phys. Chem. Lett.* **2016**, *7*, 1518.
[27] M. Cuisinier, P. E. Cabelguen, S. Evers, G. He, M. Kolbeck, A. Garsuch, T. Bolin, M. Balasubramanian, L. F. Nazar, *J. Phys. Chem. Lett.* **2013**, *4*, 3227.
[28] a) P. Barai, A. Mistry, P. P. Mukherjee, *Extreme Mech. Lett.* **2016**, *9*, 359; b) R. Fang, S. Zhao, Z. Sun, D. W. Wang, H. M. Cheng, F. Li, *Adv. Mater.* **2017**, *29*, 1606823.
[29] M. Safari, C. Y. Kwok, L. F. Nazar, *ACS Cent. Sci.* **2016**, *2*, 560.
[30] K. Kumaresan, Y. Mikhaylik, R. E. White, *J. Electrochem. Soc.* **2008**, *155*, A576.
[31] Y. V. Mikhaylik, J. R. Akridge, *J. Electrochem. Soc.* **2004**, *151*, A1969.
[32] Z. F. Deng, Z. A. Zhang, Y. Q. Lai, J. Liu, J. Li, Y. X. Liu, *J. Electrochem. Soc.* **2013**, *160*, A553.
[33] a) S. Wei, S. Xu, A. Agrawral, S. Choudhury, Y. Lu, Z. Tu, L. Ma, L. A. Archer, *Nat. Commun.* **2016**, *7*, 11722; b) Y. X. Wang, J. Yang, W. Lai, S. L. Chou, Q. F. Gu, H. K. Liu, D. Zhao, S. X. Dou, *J. Am. Chem. Soc.* **2016**, *138*, 16576.
[34] Y. Son, J. S. Lee, Y. Son, J. H. Jang, J. Cho, *Adv. Energy Mater.* **2015**, *5*, 1500110.
[35] A. Vizintin, L. Chabanne, E. Tchernychova, L. Arčon, L. Stievano, G. Aquilanti, M. Antonietti, T. P. Fellinger, R. Dominko, *J. Power Sources* **2017**, *344*, 208.
[36] Y. C. Lu, Q. He, H. A. Gasteiger, *J. Phys. Chem. C* **2014**, *118*, 5733.
[37] a) X. Q. Yu, H. L. Pan, Y. N. Zhou, P. Northrup, J. Xiao, S. Bak, M. Z. Liu, K. W. Nam, D. Y. Qu, J. Liu, T. P. Wu, X. Q. Yang, *Adv. Energy Mater.* **2015**, *5*, 1500072; b) K. R. Kim, S. H. Yu, Y. E. Sung, *Chem. Commun.* **2016**, *52*, 1198; c) P. Strubel, S. Thieme, C. Weller, H. Althues, S. Kaskel, *Nano Energy* **2017**, *34*, 437.
[38] a) H. J. Peng, J. Q. Huang, X. Y. Liu, X. B. Cheng, W. T. Xu, C. Z. Zhao, F. Wei, Q. Zhang, *J. Am. Chem. Soc.* **2017**, *139*, 8458; b) R. Xu, I. Belharouak, J. C. M. Li, X. F. Zhang, I. Bloom, J. Bareno, *Adv. Energy Mater.* **2013**, *3*, 833; c) D. J. Lee, M. Agostini, J. W. Park, Y. K. Sun, J. Hassoun, B. Scrosati, *ChemSusChem* **2013**, *6*, 2245.
[39] a) W. Li, H. Yao, K. Yan, G. Zheng, Z. Liang, Y. M. Chiang, Y. Cui, *Nat. Commun.* **2015**, *6*, 7436; b) X. B. Cheng, C. Yan, X. Chen, C. Guan, J. Q. Huang, H. J. Peng, R. Zhang, S. T. Yang, Q. Zhang, *Chem* **2017**, *2*, 258.
[40] J. Wang, Y. S. He, J. Yang, *Adv. Mater.* **2015**, *27*, 569.
[41] S. Xin, L. Gu, N. H. Zhao, Y. X. Yin, L. J. Zhou, Y. G. Guo, L. J. Wan, *J. Am. Chem. Soc.* **2012**, *134*, 18510.
[42] Z. Li, L. X. Yuan, Z. Q. Yi, Y. M. Sun, Y. Liu, Y. Jiang, Y. Shen, Y. Xin, Z. L. Zhang, Y. H. Huang, *Adv. Energy Mater.* **2014**, *4*, 1301473.
[43] a) S. S. Zhang, *Energies* **2014**, *7*, 4588; b) J. L. Wang, J. Yang, J. Y. Xie, N. X. Xu, *Adv. Mater.* **2002**, *14*, 963.
[44] B. C. Duan, W. K. Wang, A. B. Wang, K. G. Yuan, Z. B. Yu, H. L. Zhao, J. Y. Qiu, Y. S. Yang, *J. Mater. Chem. A* **2013**, *1*, 13261.

[45] J. Zhou, T. Qian, N. Xu, M. Wang, X. Ni, X. Liu, X. Shen, C. Yan, *Adv. Mater.* **2017**, *29*, 1701294.
[46] Y. H. Xu, Y. Wen, Y. J. Zhu, K. Gaskell, K. A. Cychosz, B. Eichhorn, K. Xu, C. S. Wang, *Adv. Funct. Mater.* **2015**, *25*, 4312.
[47] K. Xu, *Chem. Rev.* **2014**, *114*, 11503.
[48] B. Zhang, X. Qin, G. R. Li, X. P. Gao, *Energy Environ. Sci.* **2010**, *3*, 1531.
[49] A. Manthiram, X. W. Yu, S. F. Wang, *Nat. Rev. Mater.* **2017**, *2*, 16103.
[50] a) F. Croce, G. B. Appetecchi, L. Persi, B. Scrosati, *Nature* **1998**, *394*, 456; b) Y. Lin, X. Wang, J. Liu, J. D. Miller, *Nano Energy* **2017**, *31*, 478.
[51] a) X. A. Liang, Z. Y. Wen, Y. Liu, H. Zhang, L. Z. Huang, J. Jin, *J. Power Sources* **2011**, *196*, 3655; b) S. S. Jeong, Y. Lim, Y. J. Choi, G. B. Cho, K. W. Kim, H. J. Ahn, K. K. Cho, *J. Power Sources* **2007**, *174*, 745; c) J. Hassoun, B. Scrosati, *Adv. Mater.* **2010**, *22*, 5198.
[52] a) N. Kamaya, K. Homma, Y. Yamakawa, M. Hirayama, R. Kanno, M. Yonemura, T. Kamiyama, Y. Kato, S. Hama, K. Kawamoto, A. Mitsui, *Nat. Mater.* **2011**, *10*, 682; b) Y. Kato, S. Hori, T. Saito, K. Suzuki, M. Hirayama, A. Mitsui, M. Yonemura, H. Iba, R. Kanno, *Nat. Energy* **2016**, *1*, 16030.
[53] X. Y. Yao, N. Huang, F. D. Han, Q. Zhang, H. L. Wan, J. P. Mwizerwa, C. S. Wang, X. X. Xu, *Adv. Energy Mater.* **2017**, *7*, 1602923.
[54] B. B. Wu, S. Y. Wang, W. J. Evans, D. Z. Deng, J. H. Yang, J. Xiao, *J. Mater. Chem. A* **2016**, *4*, 15266.
[55] a) M. Li, Y. N. Zhang, X. L. Wang, W. Ahn, G. P. Jiang, K. Feng, G. Lui, Z. W. Chen, *Adv. Funct. Mater.* **2016**, *26*, 8408; b) Y. Yang, G. H. Yu, J. J. Cha, H. Wu, M. Vosgueritchian, Y. Yao, Z. N. Bao, Y. Cui, *ACS Nano* **2011**, *5*, 9187.
[56] T. Z. Hou, X. Chen, H. J. Peng, J. Q. Huang, B. Q. Li, Q. Zhang, B. Li, *Small* **2016**, *12*, 3283.
[57] W. Li, Q. Zhang, G. Zheng, Z. W. Seh, H. Yao, Y. Cui, *Nano Lett.* **2013**, *13*, 5534.
[58] a) X. L. Wang, G. Li, J. D. Li, Y. N. Zhang, A. Wook, A. P. Yu, Z. W. Chen, *Energy Environ. Sci.* **2016**, *9*, 2533; b) Z. Li, H. B. Wu, X. W. Lou, *Energy Environ. Sci.* **2016**, *9*, 3061; c) W. Z. Bao, D. W. Su, W. X. Zhang, X. Guo, G. X. Wang, *Adv. Funct. Mater.* **2016**, *26*, 8746; d) Z. Cui, C. Zu, W. Zhou, A. Manthiram, J. B. Goodenough, *Adv. Mater.* **2016**, *28*, 6926.
[59] T. Z. Hou, W. T. Xu, X. Chen, H. J. Peng, J. Q. Huang, Q. Zhang, *Angew. Chem., Int. Ed. Engl.* **2017**, *56*, 8178.
[60] a) G. R. Li, M. Ling, Y. F. Ye, Z. P. Li, J. H. Guo, Y. F. Yao, J. F. Zhu, Z. Lin, S. Q. Zhang, *Adv. Energy Mater.* **2015**, *5*, 1500878; b) G. R. Li, W. L. Cai, B. H. Liu, Z. P. Li, *J. Power Sources* **2015**, *294*, 187.
[61] a) Z. Yuan, H. J. Peng, T. Z. Hou, J. Q. Huang, C. M. Chen, D. W. Wang, X. B. Cheng, F. Wei, Q. Zhang, *Nano Lett.* **2016**, *16*, 519; b) H. J. Peng, G. Zhang, X. Chen, Z. W. Zhang, W. T. Xu, J. Q. Huang, Q. Zhang, *Angew. Chem., Int. Ed. Engl.* **2016**, *55*, 12990; c) G. Zhou, H. Tian, Y. Jin, X. Tao, B. Liu, R. Zhang, Z. W. Seh, D. Zhuo, Y. Liu, J. Sun, J. Zhao, C. Zu, D. S. Wu, Q. Zhang, Y. Cui, *Proc. Natl. Acad. Sci. USA* **2017**, *114*, 840; d) C. Zheng, S. Z. Niu, W. Lv, G. M. Zhou, J. Li, S. X. Fan, Y. Q. Deng, Z. Z. Pan, B. H. Li, F. Y. Kang, Q. H. Yang, *Nano Energy* **2017**, *33*, 306; e) H. B. Lin, L. Q. Yang, X. Jiang, G. C. Li, T. R. Zhang, Q. F. Yao, G. W. Zheng, J. Y. Lee, *Energy Environ. Sci.* **2017**, *10*, 1476.
[62] a) H. J. Peng, J. Q. Huang, X. B. Cheng, Q. Zhang, *Adv. Energy Mater.* **2017**, *7*, 1700260; b) D. H. Liu, C. Zhang, G. M. Zhou, W. Lv, G. W. Ling, L. J. Zhi, Q. H. Yang, *Adv. Sci.* **2018**, *5*, 1700270.
[63] W. J. Chung, J. J. Griebel, E. T. Kim, H. Yoon, A. G. Simmonds, H. J. Ji, P. T. Dirlam, R. S. Glass, J. J. Wie, N. A. Nguyen, B. W. Guralnick, J. Park, A. Somogyi, P. Theato, M. E. Mackay, Y. E. Sung, K. Char, J. Pyun, *Nat. Chem.* **2013**, *5*, 518.
[64] a) S. N. Talapaneni, T. H. Hwang, S. H. Je, O. Buyukcakir, J. W. Choi, A. Coskun, *Angew. Chem., Int. Ed. Engl.* **2016**, *55*, 3106; b) S. H. Je, H. J. Kim, J. Kim, J. W. Choi, A. Coskun, *Adv. Funct. Mater.* **2017**, *27*, 1703947.
[65] N. Xu, T. Qian, X. Liu, J. Liu, Y. Chen, C. Yan, *Nano Lett.* **2017**, *17*, 538.
[66] a) L. Cheng, L. A. Curtiss, K. R. Zavadil, A. A. Gewirth, Y. Y. Shao, K. G. Gallagher, *ACS Energy Lett.* **2016**, *1*, 503; b) G. R. Li, Z. P. Li, B. Zhang, Z. Lin, *Frontiers Energy Res.* **2015**, *3*, 5.
[67] a) N. Azimi, Z. Xue, I. Bloom, M. L. Gordin, D. Wang, T. Daniel, C. Takoudis, Z. Zhang, *ACS Appl. Mater. Interfaces* **2015**, *7*, 9169; b) S. Gu, R. Qian, J. Jin, Q. Wang, J. Guo, S. Zhang, S. Zhuo, Z. Wen, *Phys. Chem. Chem. Phys.* **2016**, *18*, 29293; c) S. Chen, Z. Yu, M. L. Gordin, R. Yi, J. Song, D. Wang, *ACS Appl. Mater. Interfaces* **2017**, *9*, 6959; d) W. Weng, V. G. Pol, K. Amine, *Adv. Mater.* **2013**, *25*, 1608; e) H. Lu, Y. Yuan, K. Zhang, F. R. Qin, Y. Q. Lai, Y. X. Liu, *J. Electrochem. Soc.* **2015**, *162*, A1460; f) C. X. Zu, N. Azimi, Z. C. Zhang, A. Manthiram, *J. Mater. Chem. A* **2015**, *3*, 14864.
[68] a) M. Cuisinier, P. E. Cabelguen, B. D. Adams, A. Garsuch, M. Balasubramanian, L. F. Nazar, *Energy Environ. Sci.* **2014**, *7*, 2697; b) C. W. Lee, Q. Pang, S. Ha, L. Cheng, S. D. Han, K. R. Zavadil, K. G. Gallagher, L. F. Nazar, M. Balasubramanian, *ACS Cent. Sci.* **2017**, *3*, 605.
[69] A. Shyamsunder, W. Beichel, P. Klose, Q. Pang, H. Scherer, A. Hoffmann, G. K. Murphy, I. Krossing, L. F. Nazar, *Angew. Chem., Int. Ed. Engl.* **2017**, *56*, 6192.
[70] H. L. Pan, X. L. Wei, W. A. Henderson, Y. Y. Shao, J. Z. Chen, P. Bhattacharya, J. Xiao, J. Liu, *Adv. Energy Mater.* **2015**, *5*, 1500113.
[71] L. Suo, Y. S. Hu, H. Li, M. Armand, L. Chen, *Nat. Commun.* **2013**, *4*, 1481.
[72] K. Dokko, N. Tachikawa, K. Yamauchi, M. Tsuchiya, A. Yamazaki, E. Takashima, J. W. Park, K. Ueno, S. Seki, N. Serizawa, M. Watanabe, *J. Electrochem. Soc.* **2013**, *160*, A1304.
[73] J. Scheers, S. Fantini, P. Johansson, *J. Power Sources* **2014**, *255*, 204.
[74] a) M. Liu, D. Zhou, Y. B. He, Y. Z. Fu, X. Y. Qin, C. Miao, H. D. Du, B. H. Li, Q. H. Yang, Z. Q. Lin, T. S. Zhao, F. Y. Kang, *Nano Energy* **2016**, *22*, 278; b) P. D. Frischmann, L. C. H. Gerber, S. E. Doris, E. Y. Tsai, F. Y. Fan, X. H. Qu, A. Jain, K. A. Persson, Y. M. Chiang, B. A. Helms, *Chem. Mater.* **2015**, *27*, 6765.
[75] W. Hua, Z. Yang, H. Nie, Z. Li, J. Yang, Z. Guo, C. Ruan, X. Chen, S. Huang, *ACS Nano* **2017**, *11*, 2209.
[76] S. Y. Bai, X. Z. Liu, K. Zhu, S. C. Wu, H. S. Zhou, *Nat. Energy* **2016**, *1*, 16094.
[77] a) J. Q. Huang, Q. Zhang, H. J. Peng, X. Y. Liu, W. Z. Qian, F. Wei, *Energy Environ. Sci.* **2014**, *7*, 347; b) G. R. Li, C. Wang, W. L. Cai, Z. Lin, Z. P. Li, S. Q. Zhang, *NPG Asia Mater.* **2016**, *8*, e317; c) Z. A. Ghazi, X. He, A. M. Khattak, N. A. Khan, B. Liang, A. Iqbal, J. Wang, H. Sin, L. Li, Z. Tang, *Adv. Mater.* **2017**, *29*, 1606817.
[78] L. Wang, Y. G. Wang, Y. Y. Xia, *Energy Environ. Sci.* **2015**, *8*, 1551.
[79] Y. Xiang, J. Li, J. Lei, D. Liu, Z. Xie, D. Qu, K. Li, T. Deng, H. Tang, *ChemSusChem* **2016**, *9*, 3023.
[80] a) T. Zhao, Y. Ye, X. Peng, G. Divitini, H. K. Kim, C. Y. Lao, P. R. Coxon, K. Xi, Y. J. Liu, C. Ducati, R. J. Chen, R. V. Kumar, *Adv. Funct. Mater.* **2016**, *26*, 8418; b) T. H. Zhou, W. Lv, J. Li, G. M. Zhou, Y. Zhao, S. X. Fan, B. L. Liu, B. H. Li, F. Y. Kang, Q. H. Yang, *Energy Environ. Sci.* **2017**, *10*, 1694.
[81] J. H. Kim, G. Y. Jung, Y. H. Lee, J. H. Kim, S. Y. Lee, S. K. Kwak, S. Y. Lee, *Nano Lett.* **2017**, *17*, 2220.
[82] J. Park, B. C. Yu, J. S. Park, J. W. Choi, C. Kim, Y. E. Sung, J. B. Goodenough, *Adv. Energy Mater.* **2017**, *7*, 1602567.
[83] H. J. Peng, Z. W. Zhang, J. Q. Huang, G. Zhang, J. Xie, W. T. Xu, J.L. Shi, X. Chen, X. B. Cheng, Q. Zhang, *Adv. Mater.* **2016**, *28*, 9551.

[84] T. Zhao, Y. Ye, C. Y. Lao, G. Divitini, P. R. Coxon, X. Peng, X. He, H. K. Kim, K. Xi, C. Ducati, R. Chen, Y. Liu, S. Ramakrishna, R. V. Kumar, *Small* **2017**, *13*, 1700357.
[85] R. G. Cao, W. Xu, D. P. Lv, J. Xiao, J. G. Zhang, *Adv. Energy Mater.* **2015**, *5*, 1402273.
[86] a) S. S. Zhang, *Electrochim. Acta* **2012**, *70*, 344; b) F. Wu, J. T. Lee, N. Nitta, H. Kim, O. Borodin, G. Yushin, *Adv. Mater.* **2015**, *27*, 101.
[87] A. C. Kozen, C. F. Lin, A. J. Pearse, M. A. Schroeder, X. Han, L. Hu, S. B. Lee, G. W. Rubloff, M. Noked, *ACS Nano* **2015**, *9*, 5884.
[88] C. Huang, J. Xiao, Y. Y. Shao, J. M. Zheng, W. D. Bennett, D. P. Lu, L. V. Saraf, M. Engelhard, L. W. Ji, J. G. Zhang, X. L. Li, G. L. Graff, J. Liu, *Nat. Commun.* **2014**, *5*, 3015.
[89] D. Aurbach, E. Pollak, R. Elazari, G. Salitra, C. S. Kelley, J. Affinito, *J. Electrochem. Soc.* **2009**, *156*, A694.
[90] S. Z. Xiong, K. Xie, Y. Diao, X. B. Hong, *J. Power Sources* **2013**, *236*, 181.
[91] a) X. B. Cheng, C. Yan, H. J. Peng, J. Q. Huang, S. T. Yang, Q. Zhang, *Energy Storage Mater.* **2017**, *10*, 199; b) L. Zhang, M. Ling, J. Feng, L. Q. Mai, G. Liu, J. H. Guo, *Energy Storage Mater.* **2018**, *11*, 24.
[92] C. Yan, X. B. Cheng, C. Z. Zhao, J. Q. Huang, S. T. Yang, Q. Zhang, *J. Power Sources* **2016**, *327*, 212.
[93] G. Li, Y. Gao, X. He, Q. Huang, S. Chen, S. H. Kim, D. Wang, *Nat. Commun.* **2017**, *8*, 850.
[94] Y. Yang, M. T. Mcdowell, A. Jackson, J. J. Cha, S. S. Hong, Y. Cui, *Nano Lett.* **2010**, *10*, 1486.
[95] a) W. Cai, J. Zhou, G. Li, K. Zhang, X. Liu, C. Wang, H. Zhou, Y. Zhu, Y. Qian, *ACS Appl. Mater. Interfaces* **2016**, *8*, 27679; b) J. Hassoun, B. Scrosati, *Angew. Chem., Int. Ed. Engl.* **2010**, *49*, 2371.
[96] X. L. Zhang, W. K. Wang, A. B. Wang, Y. Q. Huang, K. G. Yuan, Z. B. Yu, J. Y. Qiu, Y. S. Yang, *J. Mater. Chem. A* **2014**, *2*, 11660.
[97] a) G. Q. Tan, R. Xu, Z. Y. Xing, Y. F. Yuan, J. Lu, J. G. Wen, C. Liu, L. Ma, C. Zhan, Q. Liu, T. P. Wu, Z. L. Jian, R. S. Yassar, Y. Ren, D. J. Miller, L. A. Curtiss, X. L. Ji, K. Amine, *Nat. Energy* **2017**, *2*, 17090; b) Y. G. Li, F. J. Chen, *Nature Energy* **2017**, *2*, 17096.
[98] Y. Yang, G. Y. Zheng, Y. Cui, *Energy Environ. Sci.* **2013**, *6*, 1552.
[99] Z. J. Li, G. M. Weng, Q. L. Zou, G. T. Cong, Y. C. Lu, *Nano Energy* **2016**, *30*, 283.
[100] a) G. Zhou, E. Paek, G. S. Hwang, A. Manthiram, *Nat. Commun.* **2015**, *6*, 7760; b) H. Yao, G. Zheng, P. C. Hsu, D. Kong, J. J. Cha, W. Li, Z. W. Seh, M. T. Mcdowell, K. Yan, Z. Liang, V. K. Narasimhan, Y. Cui, *Nat. Commun.* **2014**, *5*, 3943; c) L. Qie, C. X. Zu, A. Manthiram, *Adv. Energy Mater.* **2016**, *6*, 1502459.
[101] S. Chen, F. Dai, M. L. Gordin, Z. Yu, Y. Gao, J. Song, D. Wang, *Angew. Chem., Int. Ed. Engl.* **2016**, *55*, 4231.
[102] M. Wu, Y. Cui, A. Bhargav, Y. Losovyj, A. Siegel, M. Agarwal, Y. Ma, Y. Fu, *Angew. Chem., Int. Ed. Engl.* **2016**, *55*, 10027.
[103] a) Y. Zhao, L. P. Wang, M. T. Sougrati, Z. X. Feng, Y. Leconte, A. Fisher, M. Srinivasan, Z. C. Xu, *Adv. Energy Mater.* **2017**, *7*, 1601424; b) H. L. Ye, L. Wang, S. Deng, X. Q. Zeng, K. Q. Nie, P. N. Duchesne, B. Wang, S. Liu, J. H. Zhou, F. P. Zhao, N. Han, P. Zhang, J. Zhong, X. H. Sun, Y. Y. Li, Y. G. Li, J. Lu, *Adv. Energy Mater.* **2017**, *7*, 1601602.
[104] X. Xu, W. Liu, Y. Kim, J. Cho, *Nano Today* **2014**, *9*, 604.
[105] a) Y. Mao, G. Li, Y. Guo, Z. Li, C. Liang, X. Peng, Z. Lin, *Nat. Commun.* **2017**, *8*, 14628; b) S. H. Chung, C. H. Chang, A. Manthiram, *ACS Nano* **2016**, *10*, 10462; c) Y. Z. Liu, G. R. Li, J. Fu, Z. W. Chen, X. S. Peng, *Angew. Chem., Int. Ed.* **2017**, *56*, 6176.
[106] F. Y. Fan, M. S. Pan, K. C. Lau, R. S. Assary, W. H. Woodford, L. A. Curtiss, W. C. Carter, Y. M. Chiang, *J. Electrochem. Soc.* **2016**, *163*, A3111.
[107] M. Hagen, D. Hanselmann, K. Ahlbrecht, R. Maca, D. Gerber, J. Tubke, *Adv. Energy Mater.* **2015**, *5*, 1401986.
[108] a) F. Y. Fan, Y. M. Chiang, *J. Electrochem. Soc.* **2017**, *164*, A917; b) C. Shen, J. X. Xie, M. Zhang, J. P. Zheng, M. Hendrickson, E. J. Plichta, *J. Electrochem. Soc.* **2017**, *164*, A1220.
[109] A. Jozwiuk, B. B. Berkes, T. Weiss, H. Sommer, J. Janek, T. Brezesinski, *Energy Environ. Sci.* **2016**, *9*, 2603.
[110] L. E. Camacho-Forero, T. W. Smith, S. Bertolini, P. B. Balbuena, *J. Phys. Chem. C* **2015**, *119*, 26828.
[111] a) P. A. Nelson, K. G. Gallagher, I. D. Bloom, D. W. Dees, *Modeling the Performance and Cost of Lithium-Ion Batteries for Electric-Drive Vehicles*, Argonne National Laboratory (ANL), Lemont, IL, USA **2012**; b) D. Eroglu, K. R. Zavadil, K. G. Gallagher, *J. Electrochem. Soc.* **2015**, *162*, A982; c) Z. Li, M. S. Pan, L. Su, P. C. Tsai, A. F. Badel, J. M. Valle, S. L. Eiler, K. Xiang, F. R. Brushett, Y. M. Chiang, *Joule* **2017**, *1*, 306; d) B. D. Mccloskey, *J. Phys. Chem. Lett.* **2015**, *6*, 4581.
[112] J. Chen, W. A. Henderson, H. Pan, B. R. Perdue, R. Cao, J. Z. Hu, C. Wan, K. S. Han, K. T. Mueller, J. G. Zhang, Y. Shao, J. Liu, *Nano Lett.* **2017**, *17*, 3061.
[113] C. Qu, Y. Q. Chen, X. F. Yang, H. Z. Zhang, X. F. Li, H. M. Zhang, *Nano Energy* **2017**, *39*, 262.
[114] W. J. Xue, L. X. Miao, L. Qie, C. Wang, S. Li, J. L. Wang, J. Li, *Curr. Opin. Electrochem.* **2017**, *6*, 92.
[115] F. Wu, Y. S. Ye, J. Q. Huang, T. Zhao, J. Qian, Y. Y. Zhao, L. Li, L. Wei, R. Luo, Y. X. Huang, Y. Xing, R. J. Chen, *ACS Nano* **2017**, *11*, 4694.
[116] X. B. Cheng, C. Yan, J. Q. Huang, P. Li, L. Zhu, L. D. Zhao, Y. Y. Zhang, W. C. Zhu, S. T. Yang, Q. Zhang, *Energy Storage Mater.* **2017**, *6*, 18.
[117] O. Salihoglu, R. Demir-Cakan, *J. Electrochem. Soc.* **2017**, *164*, A2948.
[118] Y. Ma, H. Zhang, B. Wu, M. Wang, X. Li, H. Zhang, *Sci. Rep.* **2015**, *5*, 14949.
[119] Oxis Energy Ltd., Jul., **2017**, https://oxisenergy.com/products/.
[120] Sion Power Corp., Mar., **2008**, http://www.sionpower.com/technology-licerion.php.
[121] Energy Gov., Nov., **2017**, https://energy.gov/eere/vehicles/batteries.

